1-1-1969

Scour at the base of spillway buckets.

D.L. Strelchuk
University of Windsor

SCOUR AT THE BASE OF SPILLWAY BUCKETS

A Thesis

Submitted to the Faculty of Graduate Studies through the
Department of Civil Engineering in Partial Fulfilment
of the Requirements for the Degree of
Master of Applied Science at the
University of Windsor

by

D.L. Strelchuk

Windsor, Ontario

1969

UMI Number: EC52776

INFORMATION TO USERS

Approved by

298209

ABSTRACT

An investigation of local scour at the base of flip buckets was conducted using gravel as the bed material with a spillway model having an ogee-type weir, an 8" bucket radius and a flip-bucket angle of 45°. Data obtained from previous studies made with a flip-bucket angle of 30° has also been incorporated.

Empirical equations are presented for maximum depth of scour, intermediate depth of scour along a radius vector originating at the point of maximum scour, radius vector length at bed level every 30° and jet trajectory length.

ACKNOWLEDGEMENTS

The author wishes to express his sincere thanks to Dr. S.P. Chee, Associate Professor in Civil Engineering, University of Windsor, for his generous assistance and guidance throughout this study.

CONTENTS

LIST OF FIGURES

LIST OF TABLES

NOMENCLATURE

Q	Discharge in cubic feet per second.
q	Discharge in cubic feet per second per foot width of spillway.
D_m	Maximum depth of scour in ft.
D	Intermediate depth of scour in ft.
d	Nominal particle size of bed material in ft.
H	Difference in elevation between upstream and tailwater level in ft.
h	Depth of tailwater in ft.
d_T	Difference in elevation between spillway lip and tailwater level in ft.
α	Flip bucket angle in radians.
V_s	Velocity in feet per second at a section through the point of maximum scour action.
g	Acceleration due to gravity in ft/sec^2.
ρ	Density in lb sec^2/ft^4.
μ	Dynamic viscosity in lb sec/ft^2.
L_J	Total jet trajectory length in ft.
L_A	Horizontal jet trajectory length in air in ft.
L_W	Horizontal jet trajectory length in water in ft.
B	Spillway width in ft.
R	Radius of the flip bucket in ft.

R_θ	Length of the radius vector at θ degrees in ft.
r	Distance of any point measured along any radius vector outwards in ft.
θ_T	Angle of jet entry into tailwater with respect to the horizontal in degrees.

CHAPTER 1

INTRODUCTION

1.1 Use of Flip Buckets

Trajectory or flip-bucket devices are used as energy dissipators at the foot of open spillways when tailwater levels in the stilling basin are insufficient for hydraulic jump formation. The bucket deflects the high velocity flows as a jet which dissipates energy in flight and lands a safe distance downstream where riverbed damage will not endanger the spillway structure. It is often used in high spillways as it is more economical than a deep and expensive hydraulic jump-type stilling basin and where hydraulic characteristics of the downstream channel are not stable enough for accurate predictions of tailwater depths in the stilling basin.

1.2 Bucket Angle

The angle of the bucket with respect to the horizontal affects the amount of energy dissipated in flight, the distance the jet will land downstream from the spillway and the maximum depth of scour in the riverbed. As the trajectory length increases the jet lands further downstream from the spillway thereby increasing energy dissipation through longer interaction of the jet with the air. With a greater exit angle the jet enters the tailwater at a steeper angle thereby increasing the vertical velocity component and directing the scouring action deeper into the channel. The net effect of a steeper angle entry into the tailwater on the scour hole configuration is to increase the maximum depth of scour and to decrease the horizontal dimensions of the scour pit.

1.3 Jet Action

After deflection from the trajectory bucket the jet falls freely through the air on a path determined by the angle of the bucket, the velocity of flow at the point of exit and the effect of air resistance. Internal turbulence, shearing action of the air surrounding the jet and surface tension are the factors determining the degree of energy dissipation in flight.

1.4 Scour Formation

When the jet enters the tailwater it has already been partially disintegrated through interaction with the surrounding air. The impact of the plunging jet however is still great enough to scour the channel bottom. At the point of impact with the bed material the turbulent eddies of the plunging jet are deflected horizontally downstream creating drag forces on the erodible material greater than the resisting forces. The scoured material is transported downstream to a point where the resisting forces are greater than the drag forces and a scour hole is gradually formed. As the scour hole deepens the degree of turbulence of the plunging jet decreases until a point of equilibrium is reached between the resisting force of the bed material and the drag force resulting in a dish shaped scour hole being formed.

1.5 Object of Investigation

The purpose of this study is to establish empirical formulae for the scour hour configuration which could enable one to predict the maximum depth of scour, the location of the scour hole and its contour pattern from the flow condition, dimensions and relative positions of spillway and basin, and bed material.

CHAPTER 2

APPARATUS AND PROCEDURE

2.1 Apparatus

The model used consisted of a spillway having an ogee-type weir, an 8" bucket radius, a flip-bucket angle of 45° and a width of 16" with a scour basin made up of 3/4" gravel having a specific gravity of 2.65. Manometers placed at the upstream and downstream ends of the basin and at the head tank were used to record water levels. Flows were recorded through the use of an electronic flow meter. The physical arrangement is shown in section and plan in Figures 1 and 2 respectively.

2.2 Procedure

Two sets of observations were conducted within a flow range of 0.76 c.f.s to 2.30 c.f.s. In the first set the flow was varied from the lowest value which would cause a measurable amount of scour in the basin to the highest value, within model limitations, to produce the maximum amount of scour. As the scour hole formed, the scoured material which was deposited directly downstream from the scour hole was removed. At the end of two hours the maximum depth of scour was measured by means of a sounding rod. As the water drained from the basin, the elevation of the receding water level was monitored with the sounding rod; strings were placed around the scour hole at 1" or 2" intervals to mark the scour hole contours.

In the second set of observations the object was to create a no scour condition or to create a condition of complete energy dissipation in the tailwater with no scour hole formation. This was accomplished by fixing the tailwater gate at a different elevation for each observation and then varying the flow for a particular observation and recording the flow at which the scouring action caused an initial displacement of the bed material.

2.3 Experimental Errors

The dial graph of the electronic flow meter was graduated in divisions of 50 USGPM resulting in graph readings of an accuracy of about 10 USGPM. Fluctuating water levels in the head tank and scour basin resulted in manometer readings being taken to the nearest 1/8". The bed level readings, because of the size of the gravel and the inherent uneveness of a composed bed could be considered accurate to the nearest 1/4".

CHAPTER 3

MAXIMUM DEPTH OF SCOUR

3.1 Factors Affecting the Maximum Depth of Scour

The maximum depth of scour was measured from the tailwater level to the bottom of the scour pit in the set of observations where scour was allowed and from the tailwater level to the top of the gravel bed in the no scour condition set of experiments.

The significant variables affecting the maximum depth (D_m) of scour are q, H, Vs, g, d, ρ, μ and α where

q = discharge in cubic feet per second per foot width of spillway

H = difference in elevation between upstream and tailwater levels

V_s = velocity in feet per second at a section through the point of maximum scour action

g = force due to gravity

d = mean diameter of the bed material

ρ = mass density of the fluid

μ = dynamic viscosity of the fluid

α = flip bucket angle in radians

The following relationship can be written:

$$f(D_m, q, H, V_s, g, d, \rho, \mu, \alpha) = 0 \tag{3.1}$$

Application of Buckingham's Theorem yields six dimensionless parameters.

$$f\left(\frac{D_m}{H}, \frac{D_m}{d}, \frac{V_s^2}{gD_m}, \frac{q}{V_s D_m}, \alpha, \frac{\rho V_s D_m}{\mu}\right) = 0 \qquad (3.2)$$

Combining dimensionless terms

$$\left(\frac{D_m}{H}\right)^{-1}\left(\frac{D_m}{d}\right) = \left(\frac{H}{d}\right) \qquad (3.3)$$

$$\left(\frac{q}{V_s D_m}\right)^2 \left(\frac{V_s^2}{gD_m}\right) \left(\frac{D_m}{H}\right)^3 = \left(\frac{q^2}{gH^3}\right) \qquad (3.4)$$

The functional relationship can be written as

$$f\left(\frac{D_m}{H}, \frac{q^2}{gH^3}, \frac{H}{d}, \alpha, \frac{\rho V_s D_m}{\mu}\right) = 0 \qquad (3.5)$$

Rearranging

$$\frac{D_m}{H} = f\left(\frac{q^2}{gH^3}, \frac{H}{d}, \alpha, \frac{\rho V_s D_m}{\mu}\right) \qquad (3.6)$$

3.2 Drop Number

The dimensionless term $\frac{q^2}{gH^3}$ formed by multiplying the Froude number with two other parameters is analagous to the 'drop number' developed for free overfall (straight drop) spillways (1).

3.3 Reynolds Number

The main disturbing force on each stone in the bed is the form drag. The Reynolds number can be used as a measure of the form drag coefficient. Beyond a value of the Reynolds number of 1000, based on the mean diameter of the gravel, the drag coefficient remains constant (2). For the correct reproduction of the drag coefficient in the model and the prototype, the Reynolds number then does not have to be equal so long as the flow is fully turbulent with the Reynolds No. greater than 1000. The model Reynolds number at the end of each observation varied from 10,700 to 25,700 with an average value of 15,400, which is well within the fully turbulent region. Since the value of the Reynolds number is greater in the prototype , its effect is even less significant and can be eliminated from the functional relationship of equation (3.6). The significant dimensionless parameters can now be written as

$$\frac{D_m}{H} = f\left(\frac{q^2}{gH^3}, \frac{H}{d}, \alpha\right) \qquad (3.7)$$

3.4 Empirical Equation for the Maximum Depth of Scour

The functional relationship of equation (3.7) can be represented in an empirical equation of the form

$$\frac{D_m}{H} = k_o\left(\frac{q^2}{gH^3}\right)^{k_1}\left(\frac{H}{d}\right)^{k_2}\left(\alpha\right)^{k_3} \qquad (3.8)$$

where K_o, K_1, K_2 and K_3 are empirical constants determined from experimental observations.

The results of Schoklitsch (3) indicate that a doubling of unit discharge increases the depth of scour by approximately 50% and that an increase in H of about six times would have to be affected to create the same increase in the depth of scour. Experimental observations presented in Table no.1 show that with a 45 degree angle flip-bucket a doubling in flow results in an approximately 50% increase in maximum depth of scour while a tripling of flow resulted in an approximate increase in the maximum depth of scour of 80%.

Based on the foregoing, and the previously stated assumptions as a premise, the following non-dimensional equation was found:

$$\frac{D_m}{H} = 3.695 \left(\frac{q^2}{gH^3}\right)^{.30} \left(\frac{H}{d}\right)^{.10} \left(\alpha\right)^{.36} \tag{3.9}$$

Simplifying

$$D_m = 1.301 \frac{q^{.60} H^{.20} \alpha^{.36}}{d^{.10}} \tag{3.10}$$

For $\alpha = 30°$,

$$D_m = 1.030 \frac{q^{.60} H^{.20}}{d^{.10}} \tag{3.11}$$

For $\alpha = 45°$,

$$D_m = 1.193 \frac{q^{.60} H^{.20}}{d^{.10}} \tag{3.12}$$

A plot of calculated versus observed values for D_m and D_m/H are presented in Figures (16) and (17) respectively.

CHAPTER 4

SCOUR HOLE CONFIGURATION

4.1 Jet Trajectory Length

The length of jet trajectory L_J is the horizontal distance between the edge of the spillway and the point of maximum depth of scour. Neglecting the effects of air resistance it is assumed that when the jet leaves the spillway it acts as a freely falling body in the air following a parabolic path having a constant horizontal velocity and a gravity accelerating vertical velocity. When the jet enters the tailwater the assumption that the effects of the surrounding fluid are negligible is no longer valid and the path of flow cannot be assumed to be totally dependent on gravity. It is assumed then that the path of the submerged jet continues on a tangent to the parabolic jet in air at the point of entry of the jet into the tailwater and also that the path of the lower nappe of the jet intersects the maximum depth of scour.

The total length of trajectory, L_J, with an initial velocity V_O is the sum of the horizontal distance the lower nappe of the jet travels up to the cross-over point of the axis of the lower nappe of the jet with the water surface, L_A, and the horizontal distance the submerged jet travels from the point of entry into the tailwater to the point of maximum depth of scour, L_W.

The initial velocity of the jet, V_O, was calculated by applying Bernoulli's equation to the upstream tank reservoir and at the base of the flip-bucket, neglecting the velocity head in the tank and assuming that the head loss due to friction between the two sections was negligible.

Taking as the centre of coordinate axes the point of exit of the jet from the spillway lip, with the ordinate positive in the upward direction the equation for the trajectory of the lower surface of the free falling nappe is

$$y = -\frac{g}{2V_O^2\cos^2\alpha} x^2 + x \tan\alpha \qquad (4.1)$$

where x and y are coordinates of any point on the lower nappe.

At the point of entry of the jet with the water surface $x = L_A$ and $y = d_T$ where d_T is the vertical distance from the lip of the flip-bucket to the tailwater level. Substituting in equation (4.1) and solving for L_A,

$$L_A = \frac{V_O^2\cos^2\alpha}{g}\left[\tan\alpha + \sqrt{\tan^2\alpha + \frac{2d_T g}{V_O^2\cos^2\alpha}}\right] \qquad (4.2)$$

After the jet enters the tailwater, the horizontal distance from the point of entry to the point of maximum depth of scour is,

$$L_W = \frac{D_T}{\tan\theta_T} \qquad (4.3)$$

where θ_T is the angle of the entry of the jet with respect to the horizontal. Taking the first derivative of y with respect to x in equation (4.1), at the point (L_A, $-d_T$),

$$\tan\theta_x = \frac{-gL_A}{V_o^2\cos^2\alpha} + \tan\alpha \tag{4.4}$$

Substituting in equation (4.3),

$$L_W = \frac{D_m}{\frac{gL_A}{V_o^2\cos^2\alpha} - \tan\alpha} \tag{4.5}$$

The total horizontal trajectory length is then

$$L_J = L_A + L_W \tag{4.6}$$

where L_A and L_W are given by equations (4.2) and (4.3) respectively.

For a flip-bucket angle of 45° and a value of g of 32.2 ft/sec^2 equations (4.2) and (4.3) reduce to

$$L_A = .0156\ V_o^2\left[1 + \sqrt{1 + \frac{128.8d_T}{V_o^2}}\right] \tag{4.7}$$

$$L_W = \frac{D_m V_o^2}{64.4L_A - V_o^2} \tag{4.8}$$

A plot of observed values of trajectory length versus calculated values is presented in Figure (28). It can be seen that for all cases the observed values are smaller than the calculated values. This is due to neglecting the effect of air resistance as a retarding factor in the jet trajectory length and the energy losses in the spillway bucket. The lowest value on the graph can be ignored since it represents the smallest flow that will exit from the bucket as a jet and as a result the frictional forces of the spillway have a disproportionate effect on the theoretical exit velocity used in the trajectory length calculation on the assumption that the frictional forces could be ignored. The remaining points indicate an observed trajectory length of about 95% the value of the calculated value. For a 45° angle flip bucket the model length of jet trajectory can then be represented by

$$L_j = .95(L_A + L_W) \quad (4.9)$$

where L_A and L_W are calculated using equations (4.7) and (4.8).

4.2 Radius Vector Lengths at Bed Level

Using the point of maximum depth of scour as origin and assuming the scour hole to be symmetrical about a reference line passing through the point of maximum depth of scour and parallel to the direction of flow empirical equations are derived for radius vector lengths at bed level at 30 degree intervals.

The significant variables that were assumed to affect the radius vector lengths are represented in the following functional relationship.

$$R_\Theta = f(B, D_m, h, H, d) \quad (4.10)$$

where R_θ = radius vector originating from the maximum depth of scour θ degrees from the reference axis with the zero degree radius vector pointing in the upstream direction and measured to the rim of the pit.

B = width of the spillway

D_m = maximum depth of scour measured from the tailwater elevation

h = depth of tailwater

d = mean diameter of the bed material

Introducing empirical parameters, a relationship of the following form may be written:

$$\frac{R_\theta}{B} = C \left(\frac{D_m-h}{h}\right)^x \left(\frac{H}{d}\right)^y \qquad (4.11)$$

where C, x and y are empirical constants.

Based on the experimental results and the work of others (4,5), the following equations for the spillway model having a 45° angle flip-bucket were obtained:

$$R_0 = 0.85\ B\left(\frac{D_m-h}{h}\right)^{0.31} \left(\frac{H}{d}\right)^{0.16} \qquad (4.12)$$

$$R_{30} = 0.81\ B\left(\frac{D_m-h}{h}\right)^{0.23} \left(\frac{H}{d}\right)^{0.16} \qquad (4.13)$$

$$R_{60} = 0.71\ B\left(\frac{D_m-h}{h}\right)^{0.31} \left(\frac{H}{d}\right)^{0.18} \qquad (4.14)$$

$$R_{90} = 0.60\ B\left(\frac{D_m-h}{h}\right)^{0.65} \left(\frac{H}{d}\right)^{.24} \qquad (4.15)$$

$$R_{120} = 0.97\, B\left(\frac{D_m - h}{h}\right)^{.93} \left(\frac{H}{d}\right)^{.15} \qquad (4.16)$$

$$R_{150} = 1.25\, B\left(\frac{D_m - h}{h}\right)^{.91} \left(\frac{H}{d}\right)^{.07} \qquad (4.17)$$

$$R_{180} = 1.29\, B\left(\frac{D_m - h}{h}\right)^{.72} \left(\frac{H}{d}\right)^{.04} \qquad (4.18)$$

A plot of calculated versus observed for the above are presented in Figures (19) to (25).

4.3 Intermediate Depths of Scour

The intermediate depth of scour D, is the vertical distance measured from a point a distance r along the radius vector R to the bottom of the scour pit below. The origin of the coordinate axes is the intersection of a plane parallel to the scour bed level with a vertical line passing through the point of maximum depth of scour; the ordinate with positive direction is taken downward, the abscissae are the directions of the radius vectors.

The functional relationship of significant variables can be written as

$$D = f(D_m, h, r, R_\Theta) \qquad (4.19)$$

Assuming that the geometric form of any scour hole profile emanating from the point of maximum depth of scour is a parabola with vertex at $(0, -D_m + h)$ the significant variables may be expressed as

$$D = (D_m - h)\left(1 - \frac{r^2}{R_\Theta^2}\right) \qquad (4.16)$$

A plot of observed values of intermediate depth of scour versus calculated values by equation (4.16) for observations of the 45° angle flip-bucket using $r/R = 1/3$ and 2/3 and for observations of the 30° angle flip-bucket (5) using $r/R = 1/4$ and $r/R = 3/4$ are shown in Figures (26) to (27) respectively.

4.4 Typical Scour Holes

A theoretical typical scour hole configuration for the 45 degree flip-bucket angle is presented in Figure (22) where q, H, h and d are given; D_m is calculated from equation (3.12); R from equations (4.12) through (4.18) and D from equation (4.16).

Similarly a theoretical typical scour hole configuration for the 30 degree flip-bucket angle is presented in Figure (23) where q, H, h and d are given, D_m is calculated from equation (3.11), R from previously developed equations (13) and D from equation (4.16).

CHAPTER 5

DISCUSSION OF RESULTS

5.1 Time for Development of Maximum Scour Condition

An important consideration for the development of maximum depth of scour is whether or not the model has operated for a length of time sufficient for its formation. Based on previous use of a similar model (5) a model run-time of two hours was chosen.

The maximum depth of scour in a non-cohesive bed material occurs when the drag forces caused by the horizontal deflection of the jet by the bed is in equilibrium with the resisting forces of the bed material. By inspection it was found that after a model running time of approximately one half hour the maximum depth of scour was formed. Beyond this time the drag forces were not great enough to transport the material out of the scour hole but were great enough to cause suspension and erratic movement of bed material within the scour hole. At the point of equilibrium then, the drag forces are sufficient to keep some of the bed material in suspension but insufficient to transport them away from the scour pit. Any further increase in the maximum depth of scour at this point would be a result of erosion of the individual particles or a reduction in particle size diameter caused by abrasion of the suspended material with the bed which would in effect decrease the resisting force of the particle to the point where the drag forces would be capable of removing it from the scour pit.

5.2 Maximum Depth of Scour

5.2.1 Flip Bucket Angle

By examining equations (3.11) and (3.12) it can be seen that the increase in the maximum depth of scour by increasing the flip bucket angle from 30° to 45° and by keeping q, H and d constant is approximately 16 percent. The increased depth is a result of the steeper angle of entry of the jet into the tailwater thereby increasing the vertical component of the scouring action and causing the jet to dig deeper into the scour bed.

5.2.2 No Scour Condition

The results of the no scour condition observations with the 45 degree angle flip bucket described in section 2.2 are given in Table 2. In this case the maximum depth of scour at equilibrium is simply the tailwater depth. From Figure(18) where the maximum depth of scour for both cases is combined, the resulting plot indicates that for a given q, H and d the maximum depth of scour would be the same whether the elevation of the gravel bed was such that a scour hole formed, or whether the gravel bed was at an elevation where no scour occurred. It would appear then that the maximum depth of scour is independent of the type of bed material, however, this is not the case since in both the scour and no scour condition, equilibrium between the drag forces and the resisting forces of the bed material exists at the final point of contact of the plunging jet and the bed. The dissipation of the energy of the jet is caused by impact with the tailwater resulting in energy dissipating turbulent eddies and by impact of the turbulent eddies with the bed material creating drag forces which act on the gravel bed with the resisting force dependent on the particle size and specific gravity of the material. If a sand bed was substituted for the gravel bed and the same q, H and d which resulted in a no scour condition in the gravel bed were applied to the sand bed, scour would form since the resisting forces of the sand particles are not as great as gravel. The scouring action would continue until an equilibrium between the two opposing forces was attained. Thus the particle size of a non-cohesive bed material is an important factor in the determination of the maximum depth of scour.

5.2.3 Other Equations for the Maximum Depth of Scour

Veronese - U.S.B.R (1), Khosla (6), and Schoklistch (7) have suggested the following equations for maximum depth of scour at equilibrium. The units are the same as those of this paper unless otherwise noted.

$$\text{Veronese-USBR}: D_m = 1.32\, q^{0.54} H^{0.225} \quad (5.1)$$

$$\text{Khosla}: D_m = K \frac{(0.9\, q^{2/3})}{f^{1/3}} \quad (5.2)$$

where $f = 8d^{1/2}$ is the Lacey silt factor and d is expressed in inches and K is an empirical coefficient with a known range of value from 1.5 to 2.1.

$$\text{Schoklitsch}: D_m = \frac{3.15\, q^{0.57} H^{0.5}}{d_{mm}^{0.32}} \quad (5.3)$$

The above equations were used to calculate the maximum depth of scour using the data of the observations of the 45 degree flip bucket angle spillway. The results are plotted in Figure (18). The calculated values are in all cases lower than the observed values. A possible explanation is the omission of the flip-bucket angle as a variable in all three equations. As previously discussed the depth of scour varies with an increase in flip-bucket angle. Assuming this to be valid each of the above equations are true for a specific angle of flip bucket which is less than 45°. Another interesting feature apparent in Figure (18) is the similarity of the plots for each particular equation.

5.3 Length of Trajectory

The model jet trajectory length given by equation (4.9) will probably not occur with prototype lengths because of the greater effect of spray formation, air resistance, and the higher velocity prototype jets experience. It has been suggested that prototype trajectory lengths are approximately 5% less than model jet trajectory lengths. (3).

5.4 Scour Hole Configuration

Typical scour holes for the 30 and 45 degree angle flip buckets plotted from the empirical equations presented in Chapter 4 are presented in Figures (29) and (30) respectively. In both cases the point of maximum scour is downstream from the geometrical centre of the scour hole with the 45 degree angle flip bucket scour hole closer to the center. This indicates that the scour hole becomes more circular as the flip-bucket angle increases.

5.5 Effect of Reynolds Number

An attempt to determine whether the basin Reynolds No. had any significant effect on the maximum scour hole depth had also been made. The scour hole Reynolds No. is defined as $V_s R/\nu$, where the velocity (V_s) and the hydraulic radius (R) refer to the cross-section where maximum scour occured. These cross-sections with the corresponding longitudinal profiles are given in Figs (10) to (15).

No positive conclusion can be drawn with regard to the influence this parameter has on the limiting scour hole depth since all model flows were within the fully turbulent region.

5.6 Application of Results

Knowing the range of spillway flows and the composition of the downstream river bed the equations presented could be used in prototype design to determine the bucket lip elevation for a no scour condition in the river bed based on the maximum depth of scour caused by the maximum design flow of the spillway and based on the corresponding tailwater depth determined by downstream channel characteristics. If the spillway lip elevation was fixed the minimum tailwater for a no scour condition could be determined.

If a no scour condition is not feasible then a pre-excavated scour hole could be provided to accommodate the scouring action of the jet. The dimensions of the pit would be dependent on the jet trajectory lengths and scour hole configurations.

Equation (3.9) includes all the significant dimensionless parameters and should have general application. An area of further study however could perhaps be the verification of the exponent for the flip-bucket angle since only two were used in this study. Application of the equations for intermediate depth of scour and radius vector lengths should be kept within the corresponding prototype flows used in the model study with the principle of superposition applied to determine prototype scour hole configuration.

5.7 Correlation Coefficients

Multiple and individual correlation coefficients for each equation presented in this study are given in Appendix G.

APPENDIX A.

Experimental Apparatus

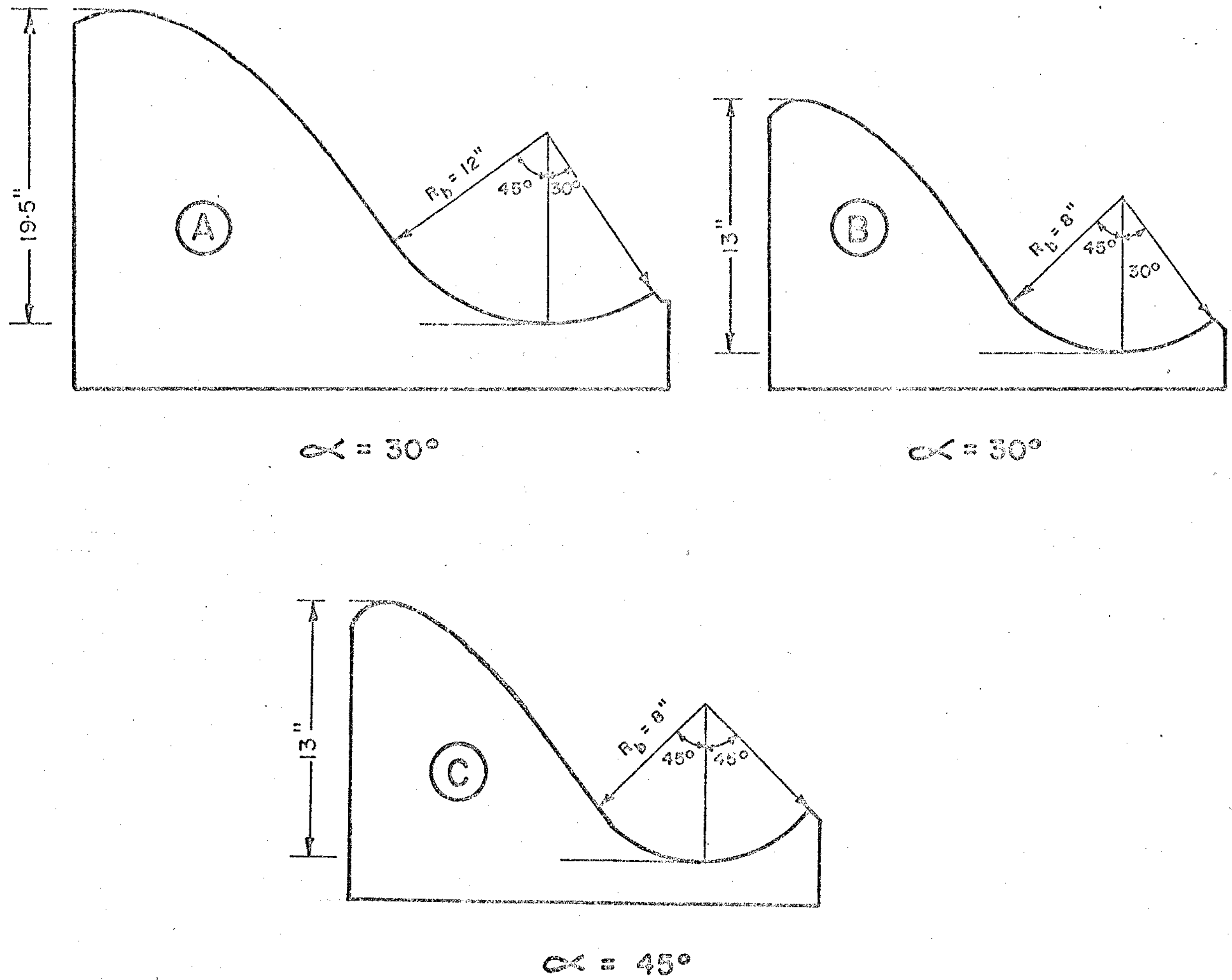

FIG. I SPILLWAYS & FLIP BUCKETS

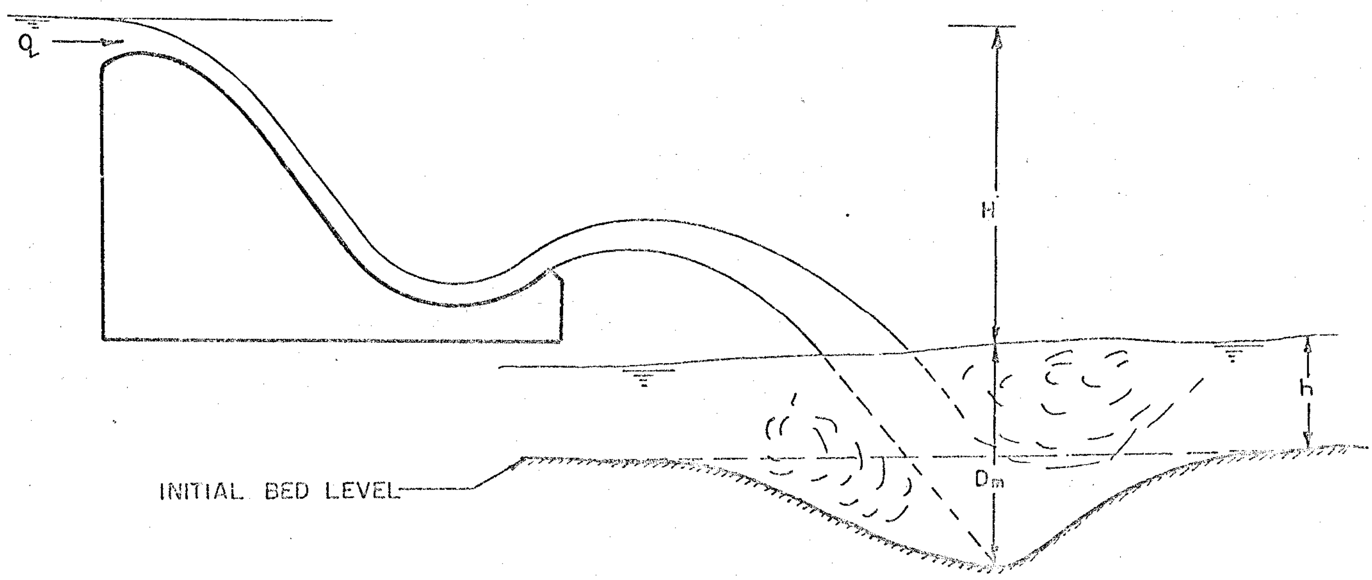

FIG. 2 SPILLWAY IN OPERATION

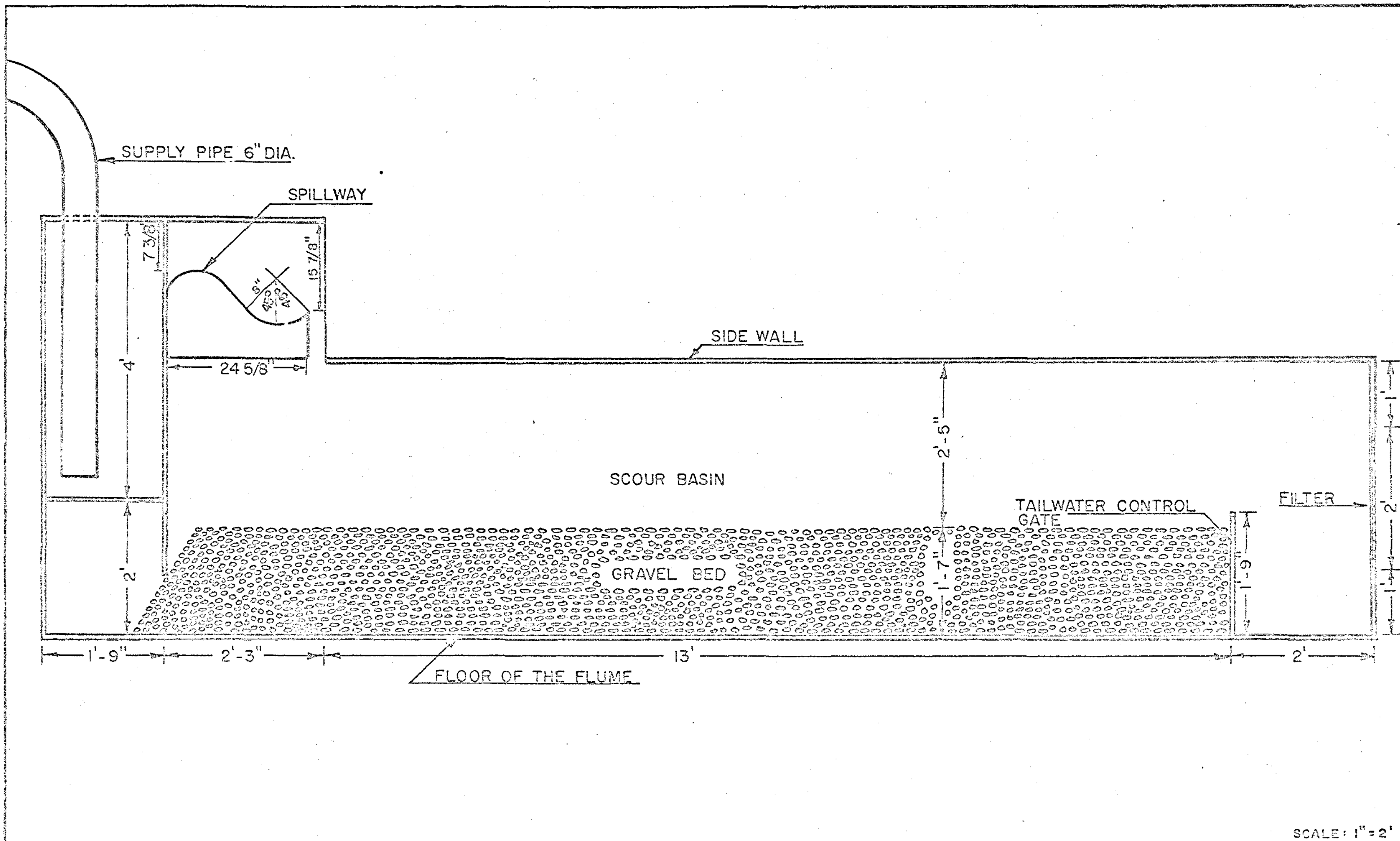

FIG.3 SECTIONAL VIEW OF EXPERIMENTAL APPARATUS

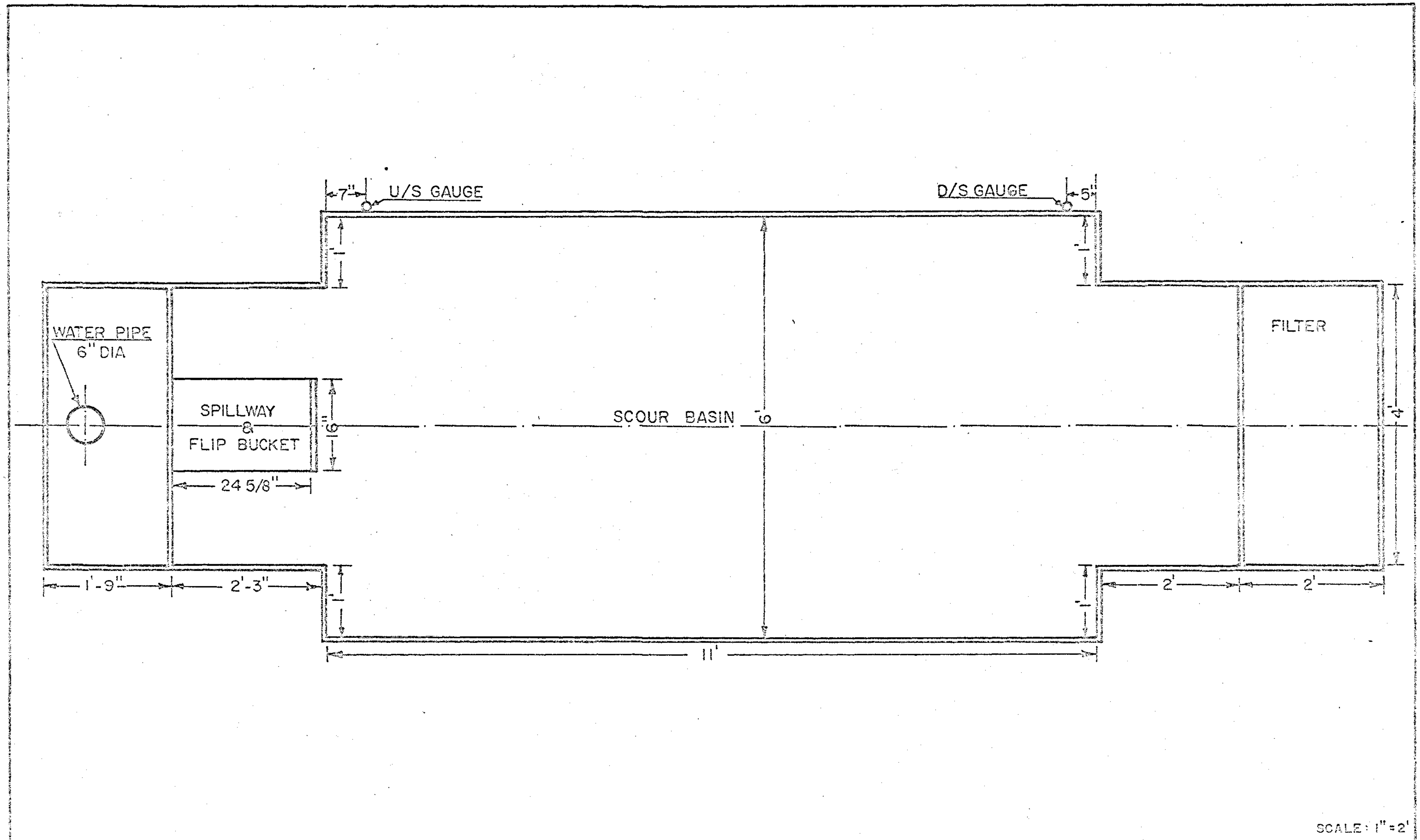

FIG.4 PLAN VIEW OF EXPERIMENTAL APPARATUS

APPENDIX B.

Scour Hole Contours

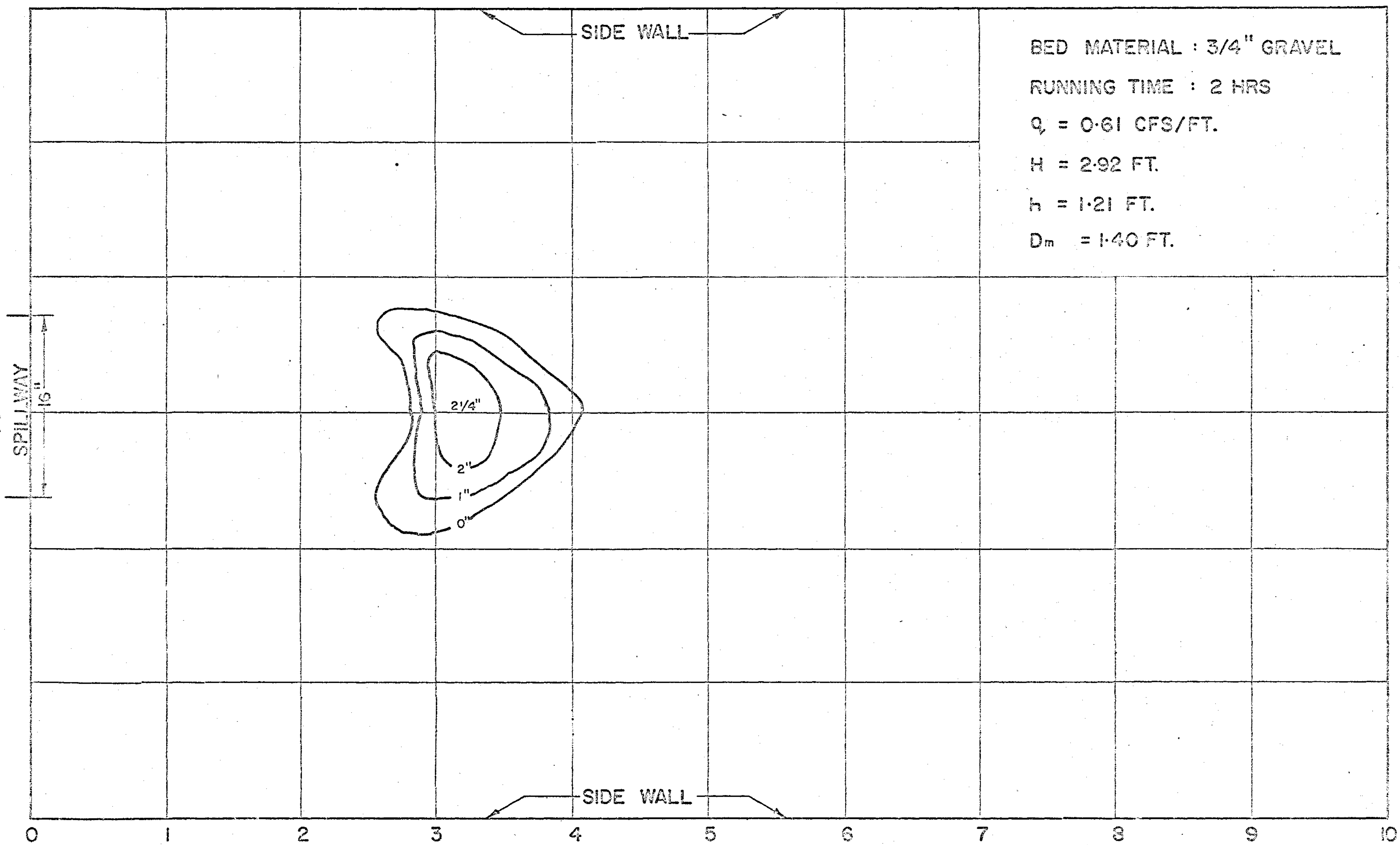

FIG.5 DISTANCE FROM DOWNSTREAM EDGE OF FLIP BUCKET. (FT.)

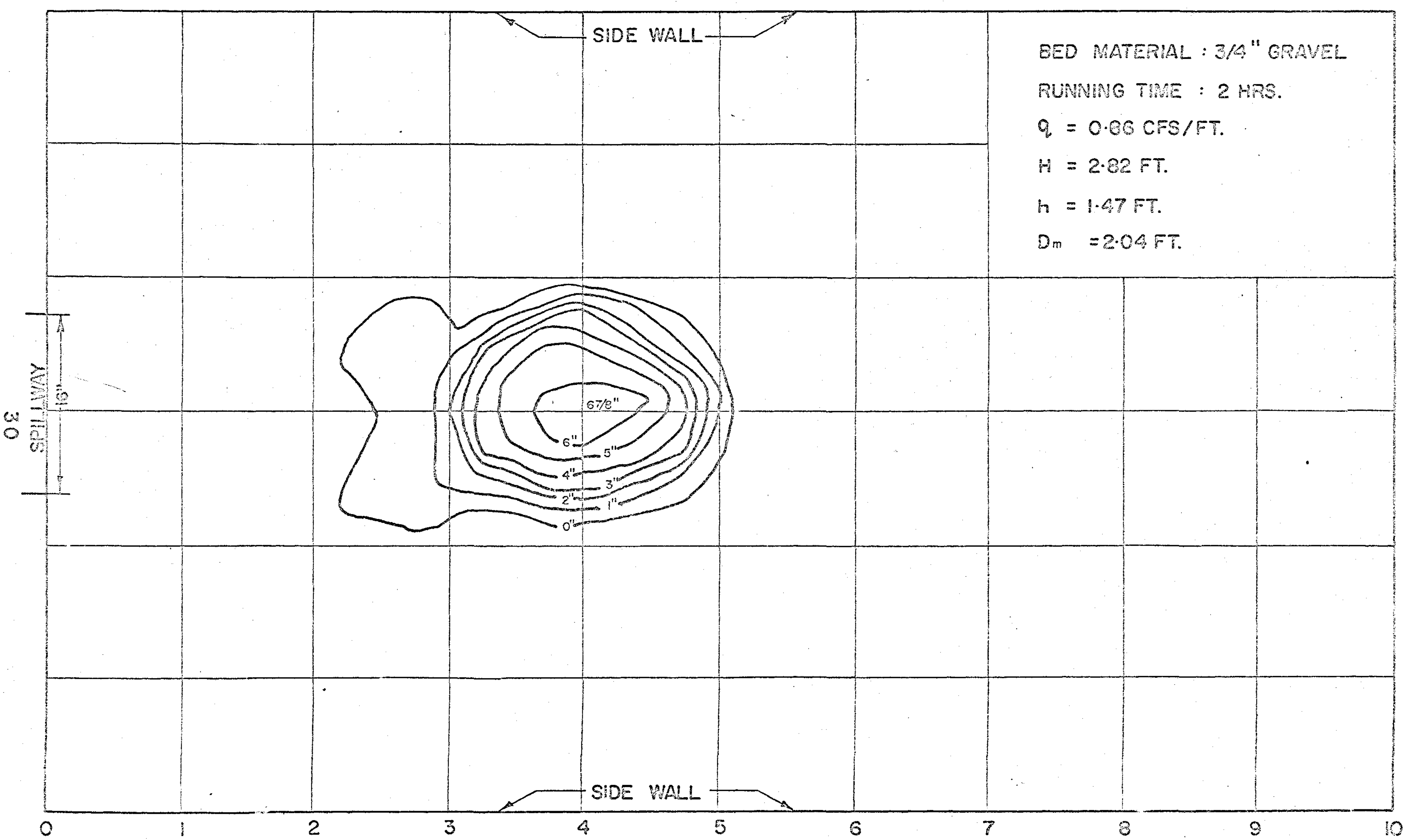

FIG.6 DISTANCE FROM DOWNSTREAM EDGE OF FLIP BUCKET. (FT.)

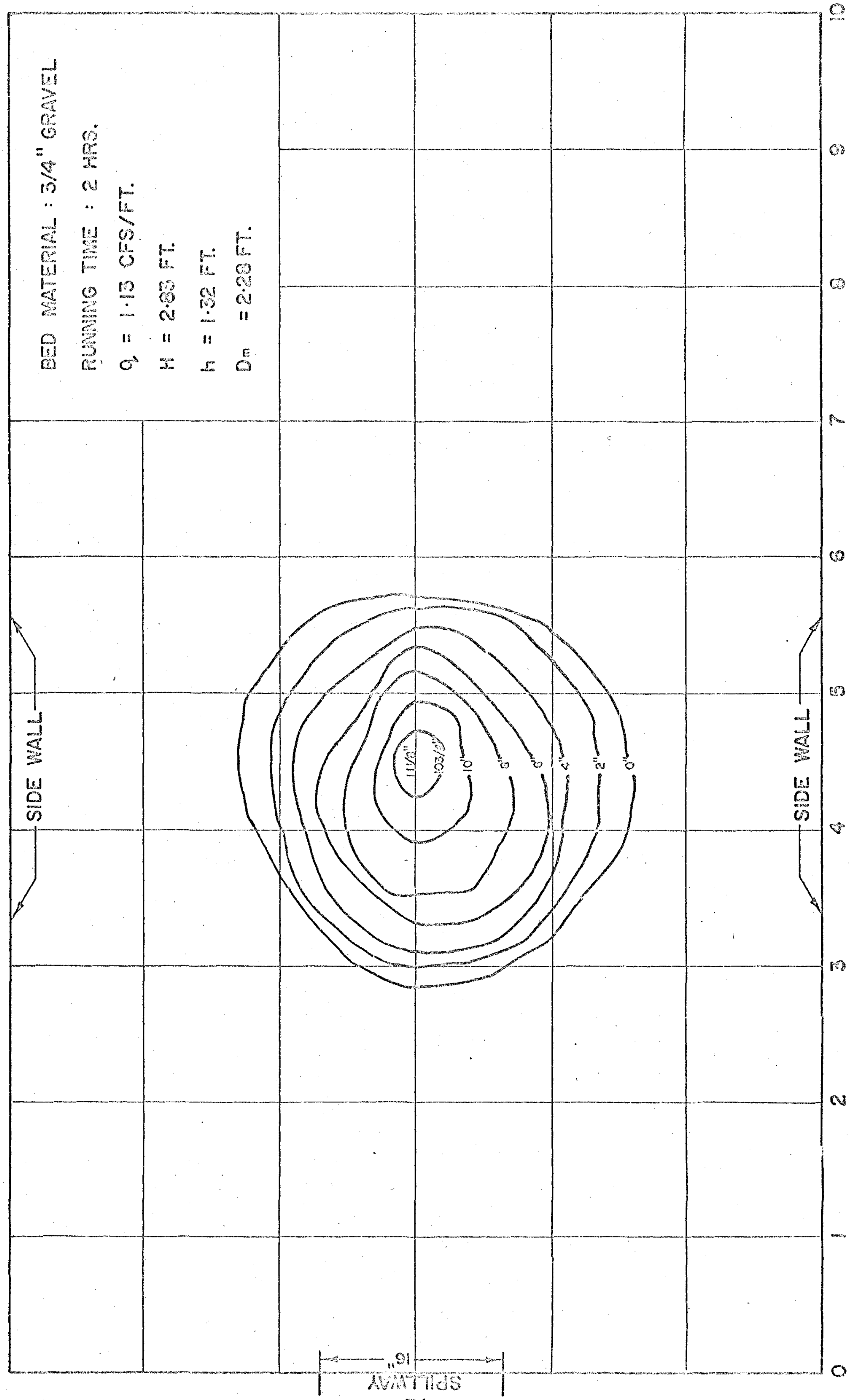

FIG. 7 DISTANCE FROM DOWNSTREAM EDGE OF FLIP BUCKET. (FT.)

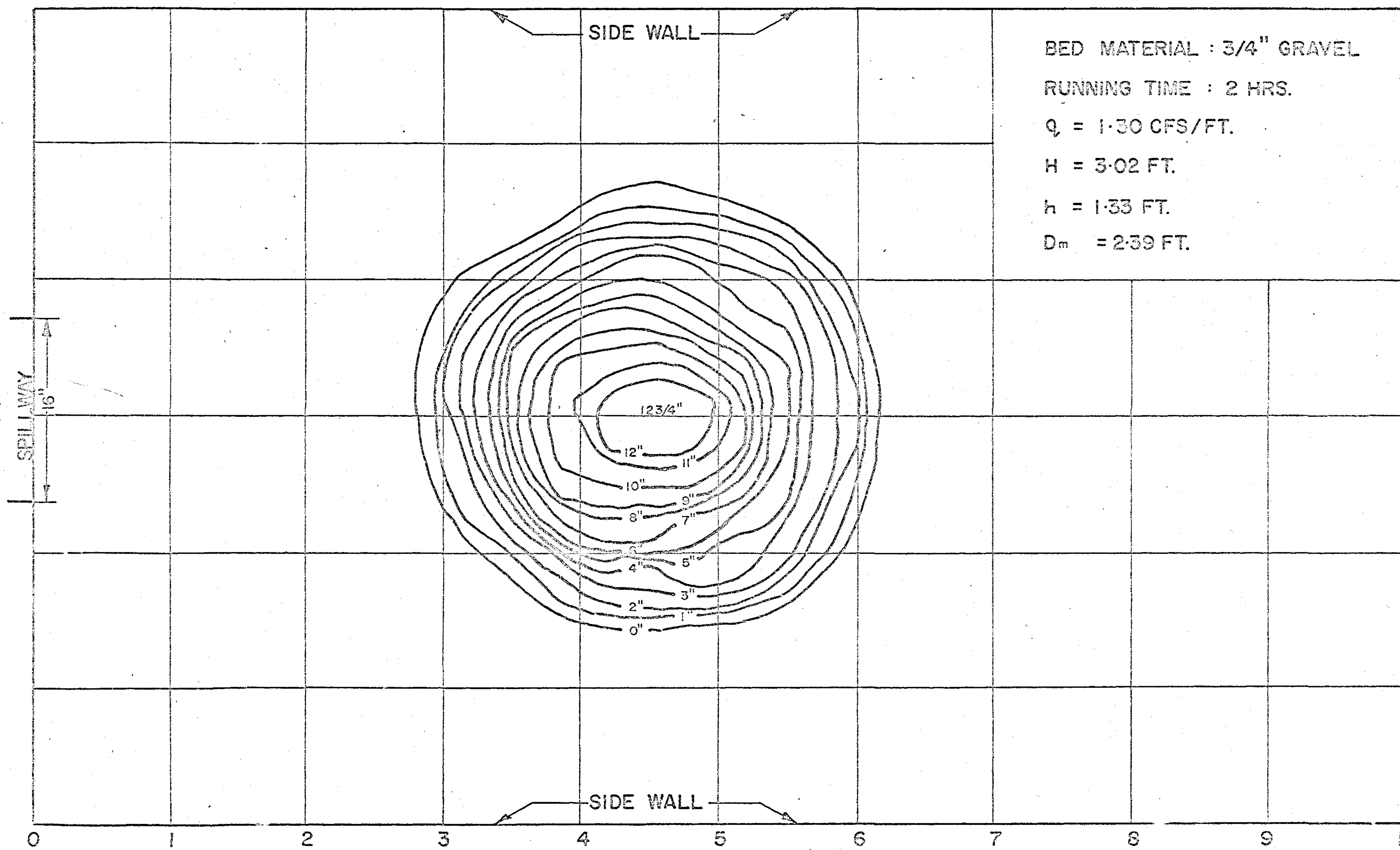

FIG. 8 DISTANCE FROM DOWNSTREAM EDGE OF FLIP BUCKET. (FT.)

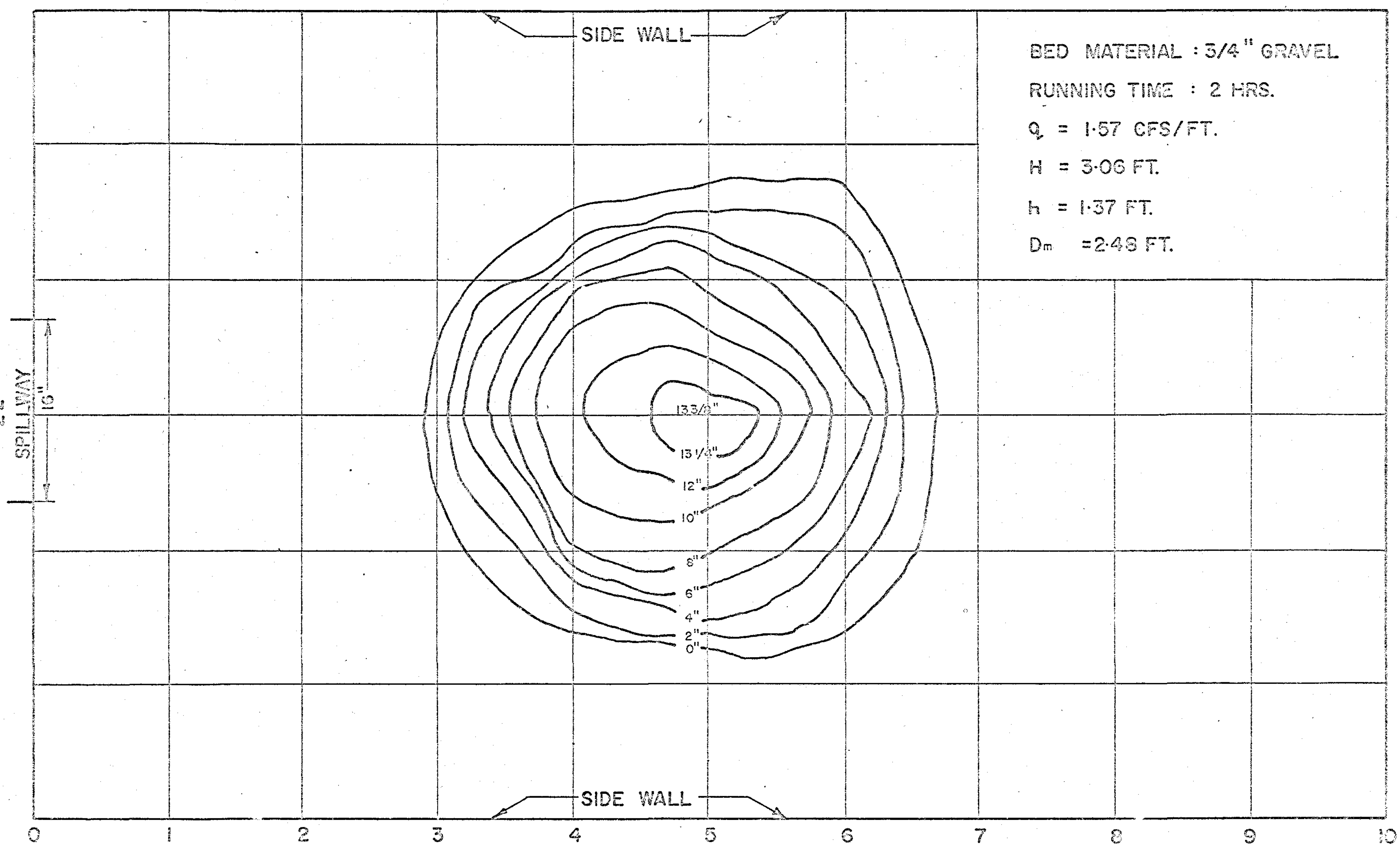

FIG.9 DISTANCE FROM DOWNSTREAM EDGE OF FLIP BUCKET. (FT.)

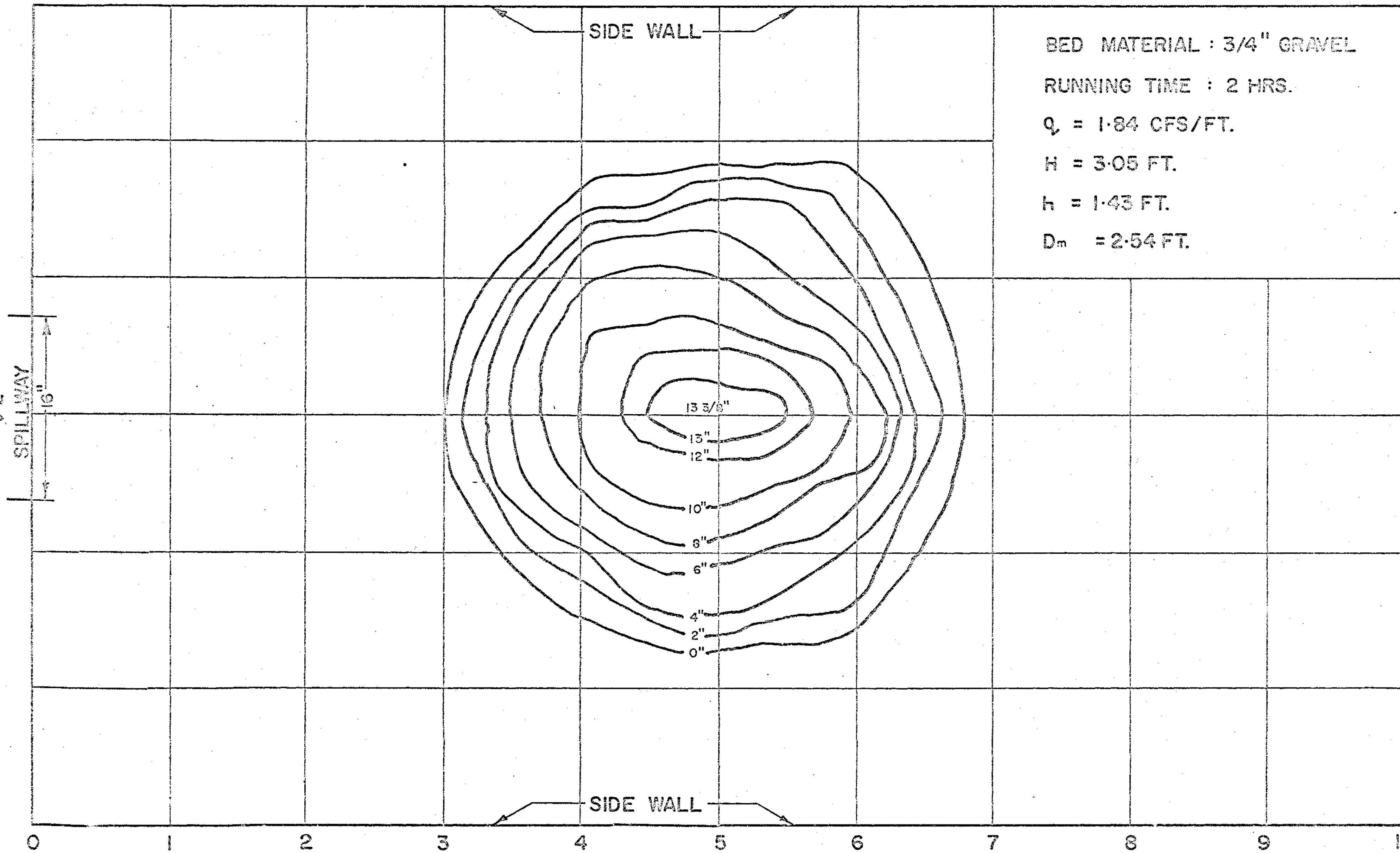

FIG.10 DISTANCE FROM DOWNSTREAM EDGE OF FLIP' BUCKET. (FT.)

APPENDIX C.

Scour Hole Cross-sections

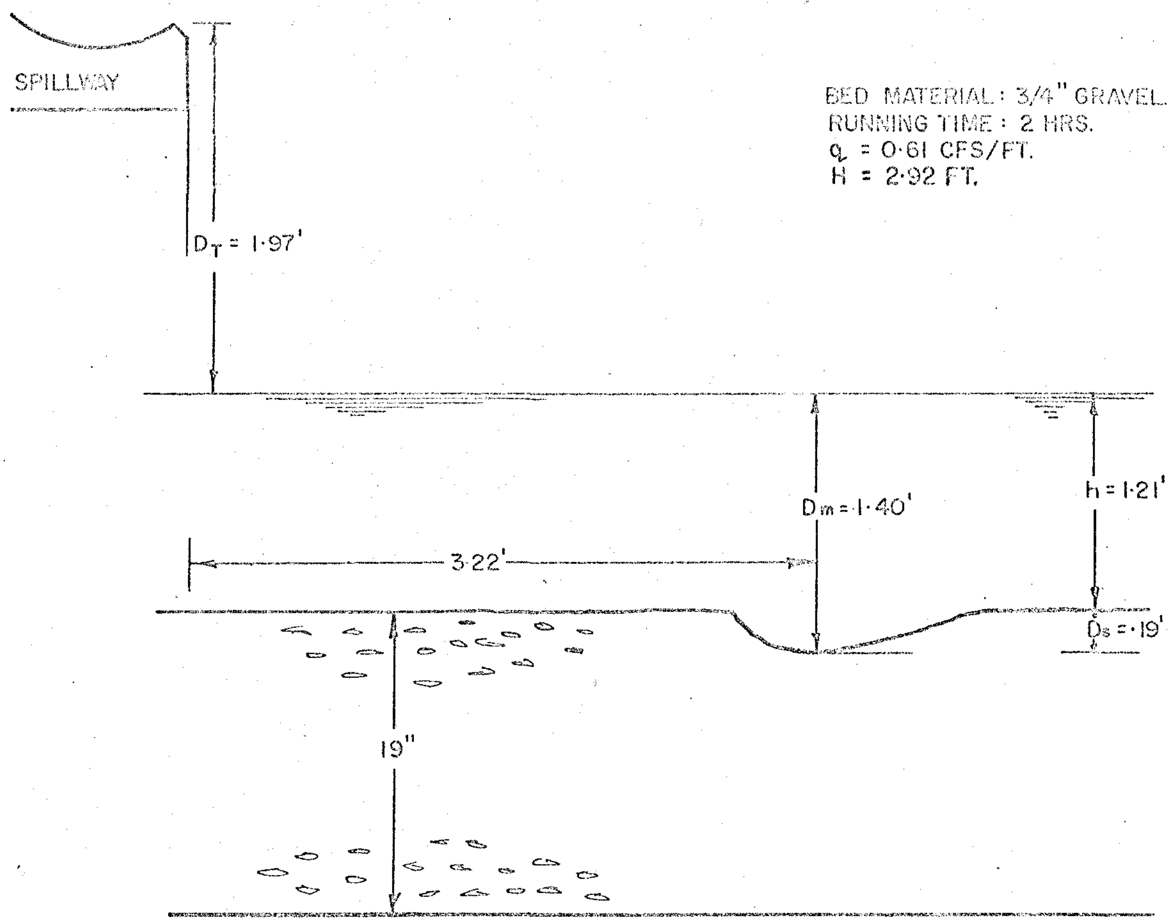

LONGITUDINAL ℄ CROSS-SECTION

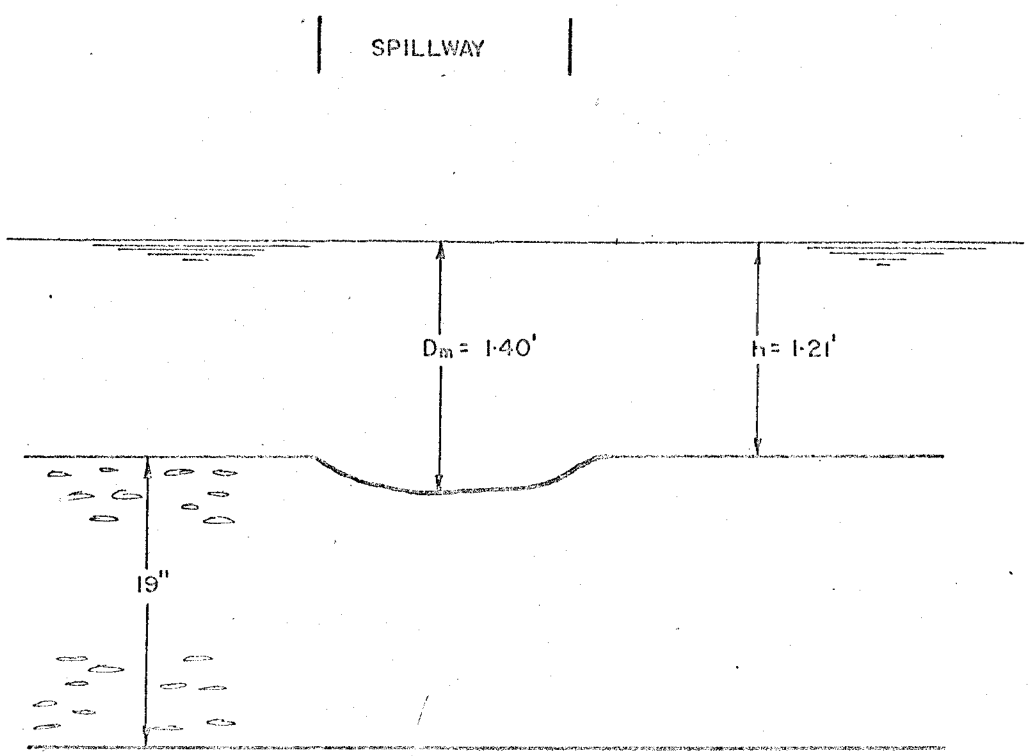

FIG. 10 TRANSVERSE ℄ CROSS-SECTION

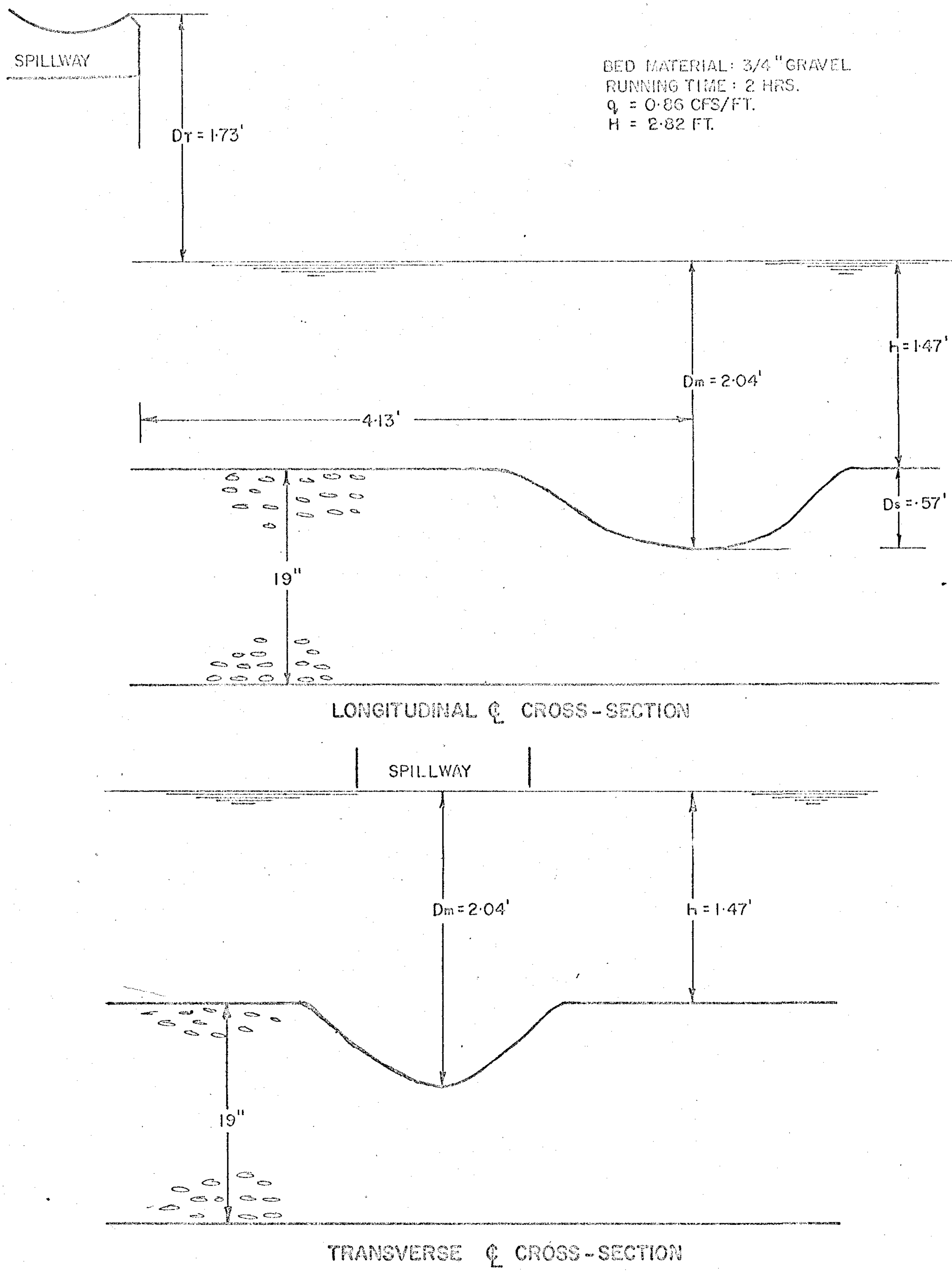
SPILLWAY
BED MATERIAL: 3/4" GRAVEL
RUNNING TIME: 2 HRS.
q = 0·86 CFS/FT.
H = 2·82 FT.
DT = 1·73'
Dm = 2·04'
h = 1·47'
4·13'
Ds = ·57'
19"
LONGITUDINAL ℄ CROSS-SECTION
SPILLWAY
Dm = 2·04'
h = 1·47'
19"
TRANSVERSE ℄ CROSS-SECTION

FIG. 11

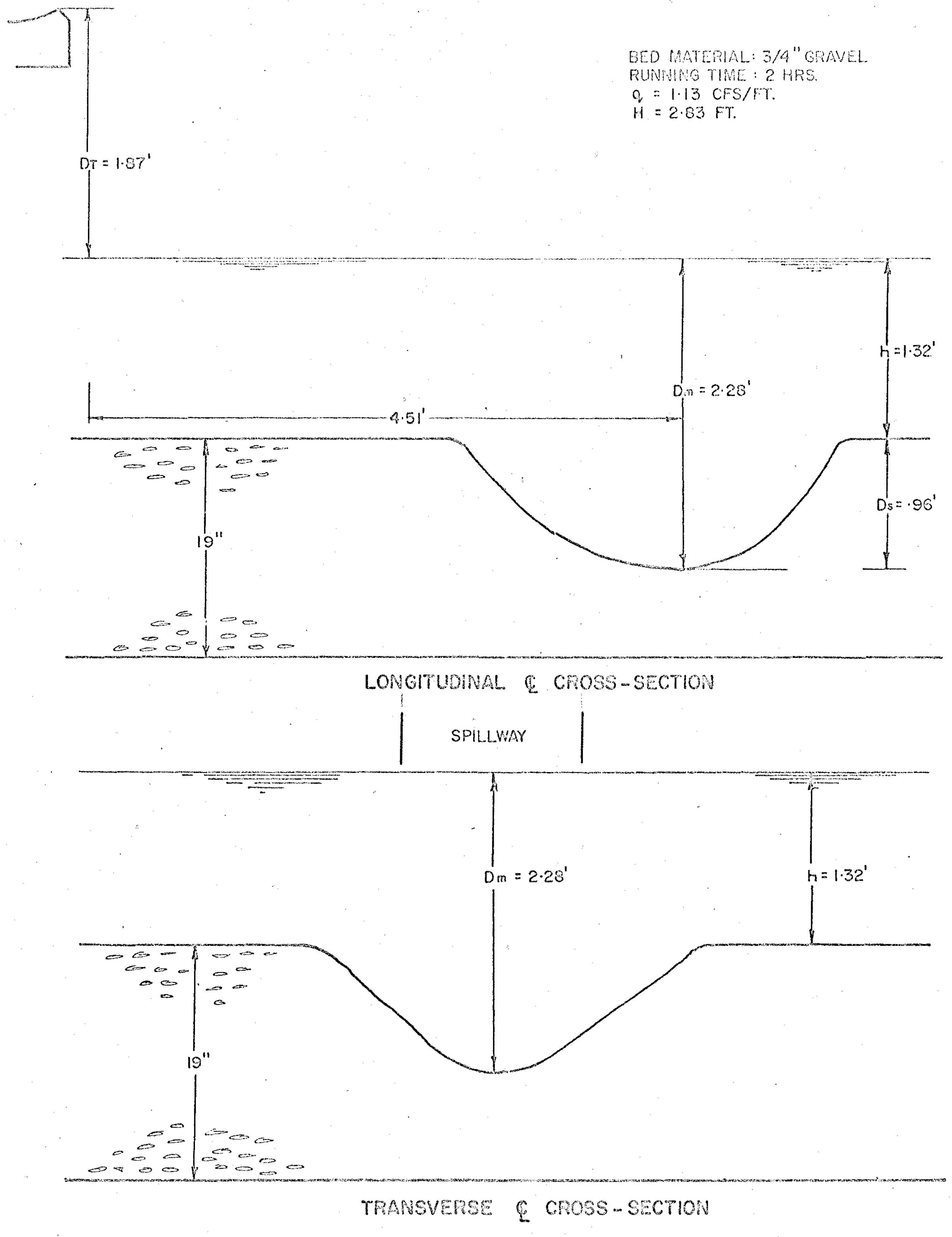

BED MATERIAL: 3/4" GRAVEL
RUNNING TIME : 2 HRS.
q = 1·13 CFS/FT.
H = 2·83 FT.
DT = 1·87'
h = 1·32'
Dm = 2·28'
4·51'
Ds = ·96'
19"
LONGITUDINAL ℄ CROSS-SECTION
SPILLWAY
Dm = 2·28'
h = 1·32'
19"
TRANSVERSE ℄ CROSS-SECTION

FIG. 12

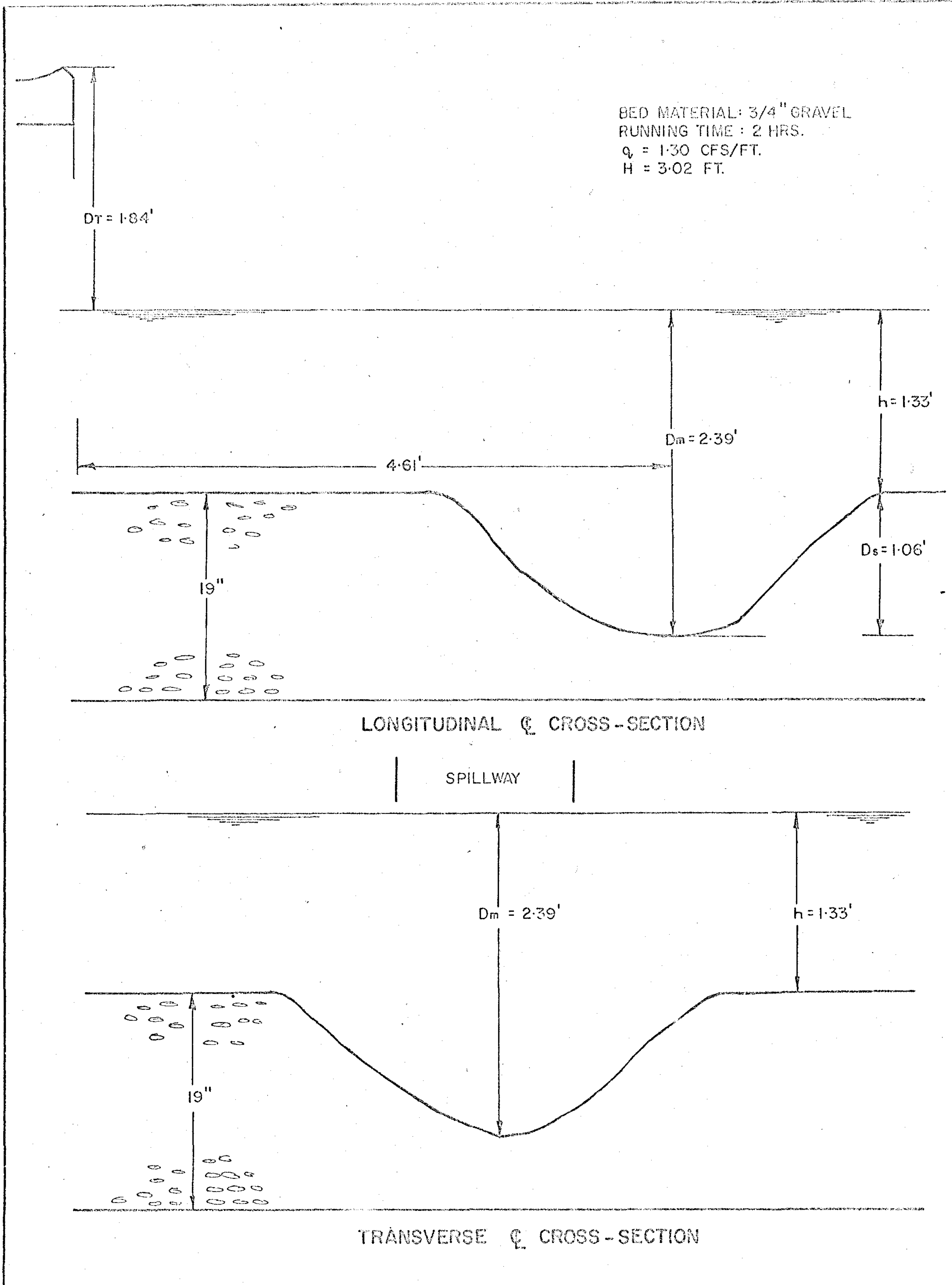
BED MATERIAL: 3/4" GRAVEL
RUNNING TIME : 2 HRS.
q = 1·30 CFS/FT.
H = 3·02 FT.
DT = 1·84'
h = 1·33'
Dm = 2·39'
4·61'
Ds = 1·06'
19"
LONGITUDINAL ℄ CROSS-SECTION
SPILLWAY
Dm = 2·39'
h = 1·33'
19"
TRANSVERSE ℄ CROSS-SECTION

FIG. 13

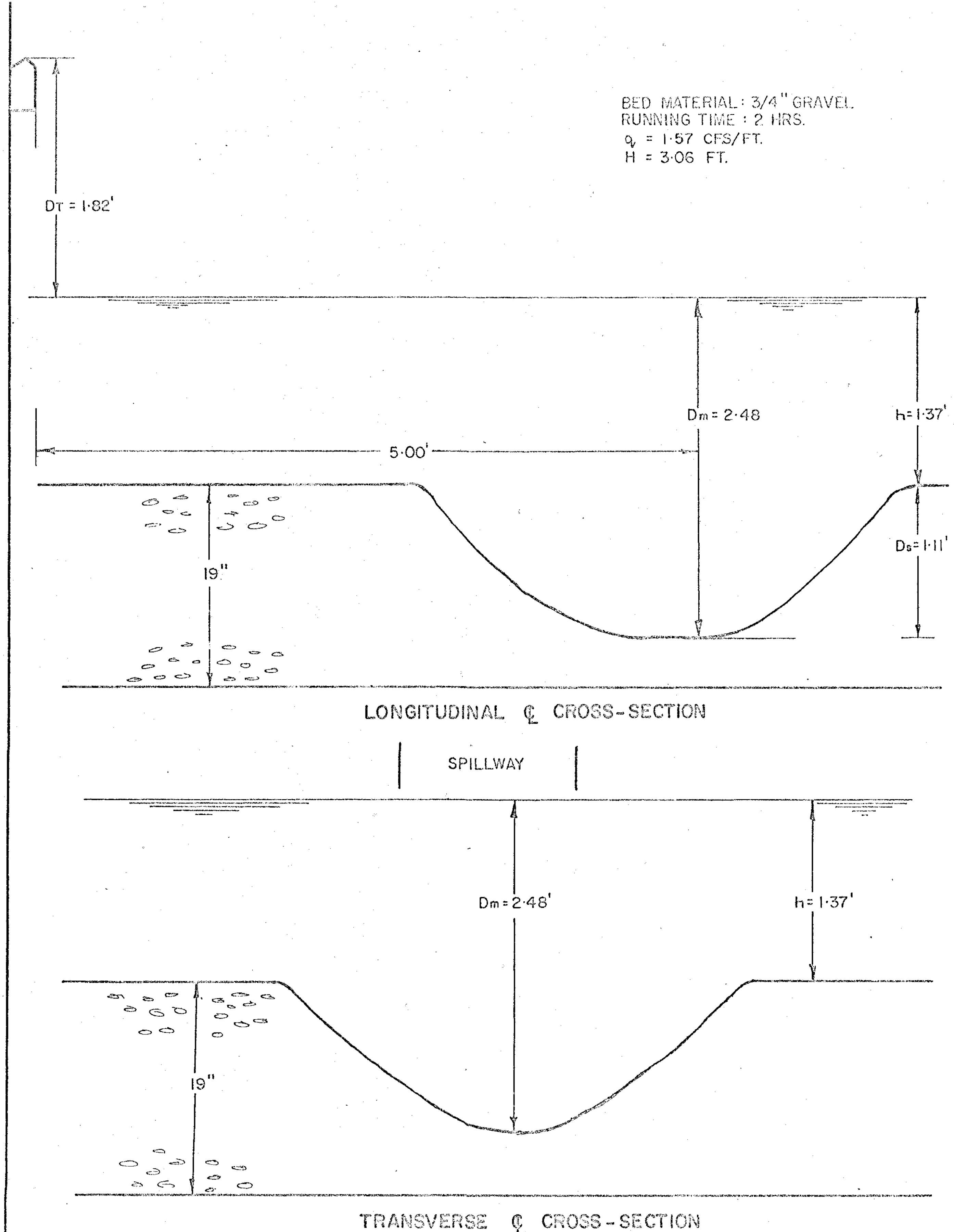

BED MATERIAL: 3/4" GRAVEL
RUNNING TIME: 2 HRS.
q = 1·57 CFS/FT.
H = 3·06 FT.
DT = 1·82'
Dm = 2·48
h = 1·37'
5·00'
Ds = 1·11'
19"
LONGITUDINAL ℄ CROSS-SECTION
SPILLWAY
Dm = 2·48'
h = 1·37'
19"
TRANSVERSE ℄ CROSS-SECTION

FIG. 14

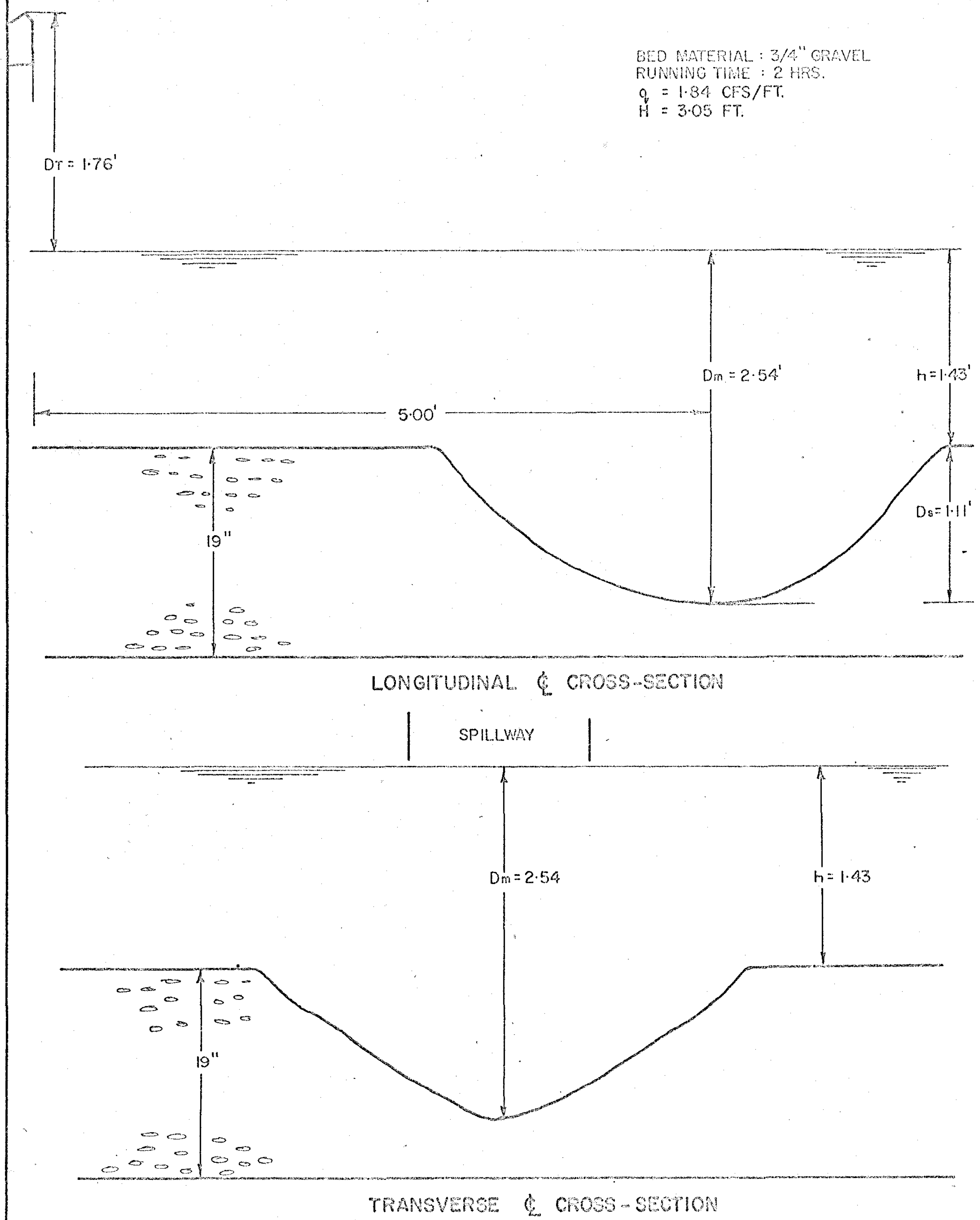

BED MATERIAL : 3/4" GRAVEL
RUNNING TIME : 2 HRS.
q = 1·84 CFS/FT.
H = 3·05 FT.
DT = 1·76'
Dm = 2·54'
h = 1·43'
5·00'
19"
Ds = 1·11'
LONGITUDINAL ℄ CROSS-SECTION
SPILLWAY
Dm = 2·54
h = 1·43
19"
TRANSVERSE ℄ CROSS-SECTION

FIG. 15

APPENDIX D.

Graphs of Observed and Calculated Values of Experimental Results

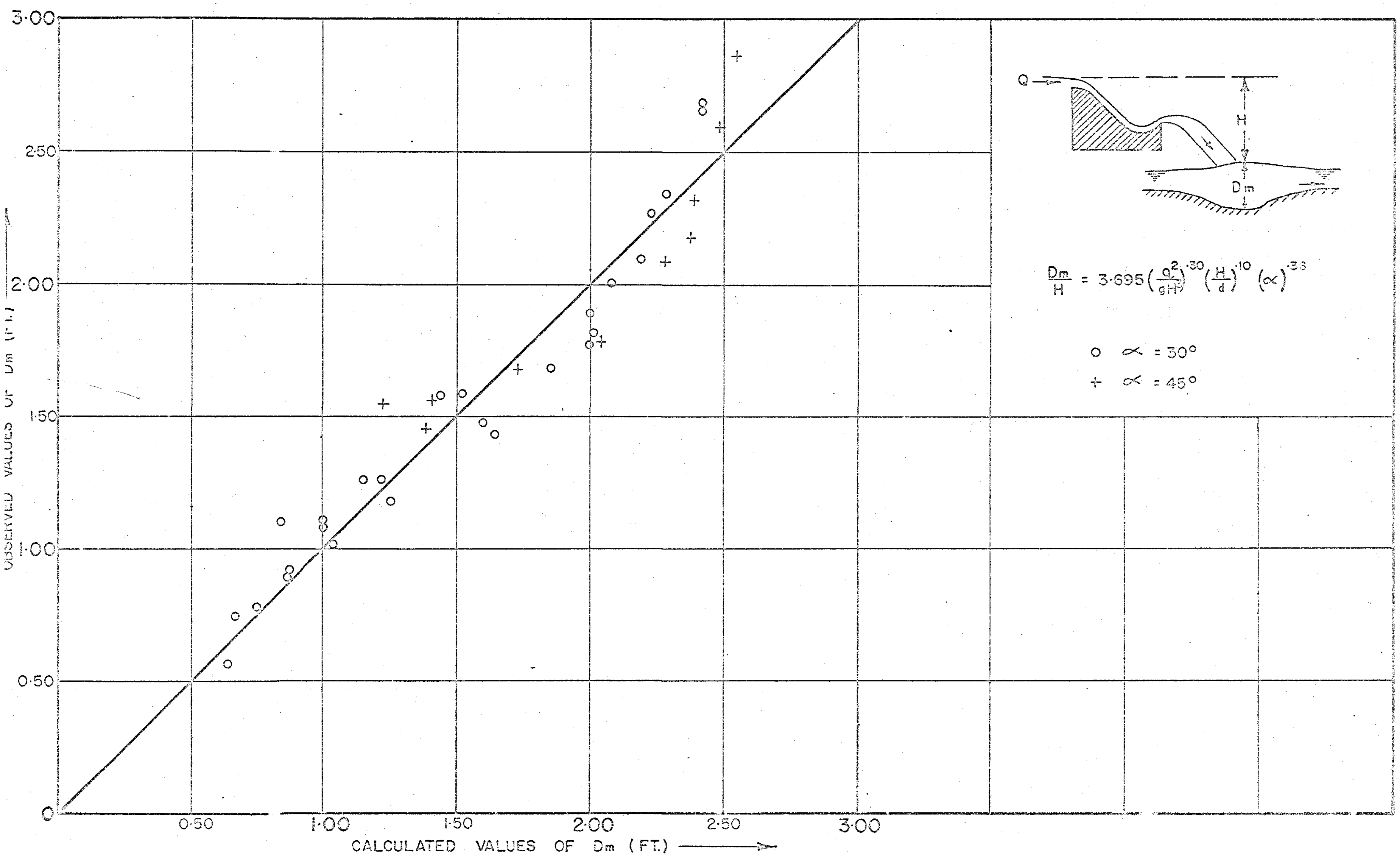

3·00
2·50
2·00
1·50
1·00
0·50
0
OBSERVED VALUES OF Dm (FT.)
0·50
1·00
1·50
2·00
2·50
3·00
CALCULATED VALUES OF Dm (FT.)
Q
H
Dm
$\frac{D_m}{H} = 3{\cdot}695\left(\frac{q^2}{gH^3}\right)^{\cdot 30}\left(\frac{H}{d}\right)^{\cdot 10}(\alpha)^{\cdot 33}$
○ α = 30°
+ α = 45°

FIG. 16

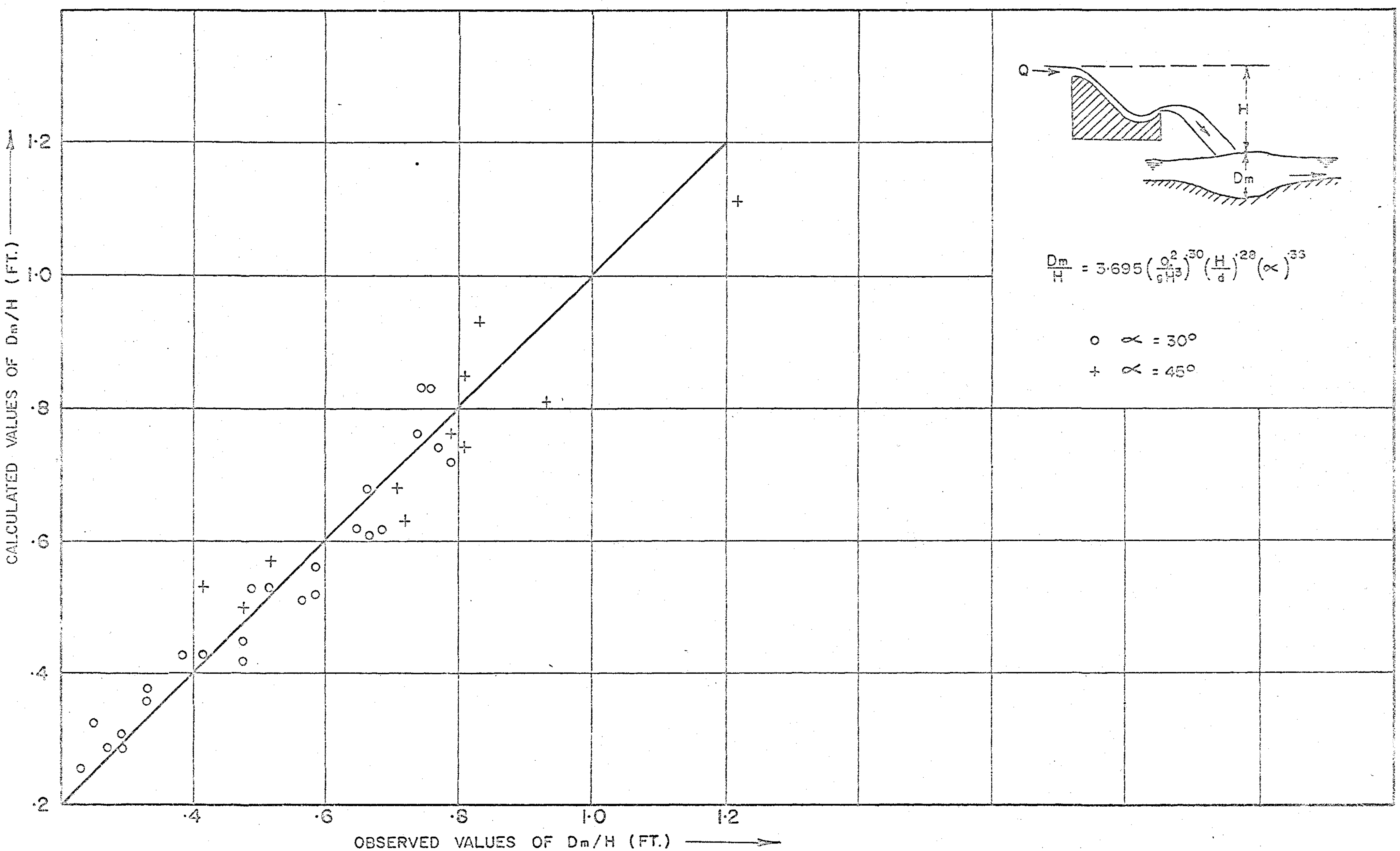
Q
H
Dm
$\frac{D_m}{H} = 3.695 \left(\frac{Q^2}{gH^3}\right)^{.30} \left(\frac{H}{d}\right)^{.28} (\alpha)^{.33}$
o α = 30°
+ α = 45°
CALCULATED VALUES OF Dm/H (FT.)
OBSERVED VALUES OF Dm/H (FT.)
·2
·4
·6
·8
1·0
1·2

FIG.17

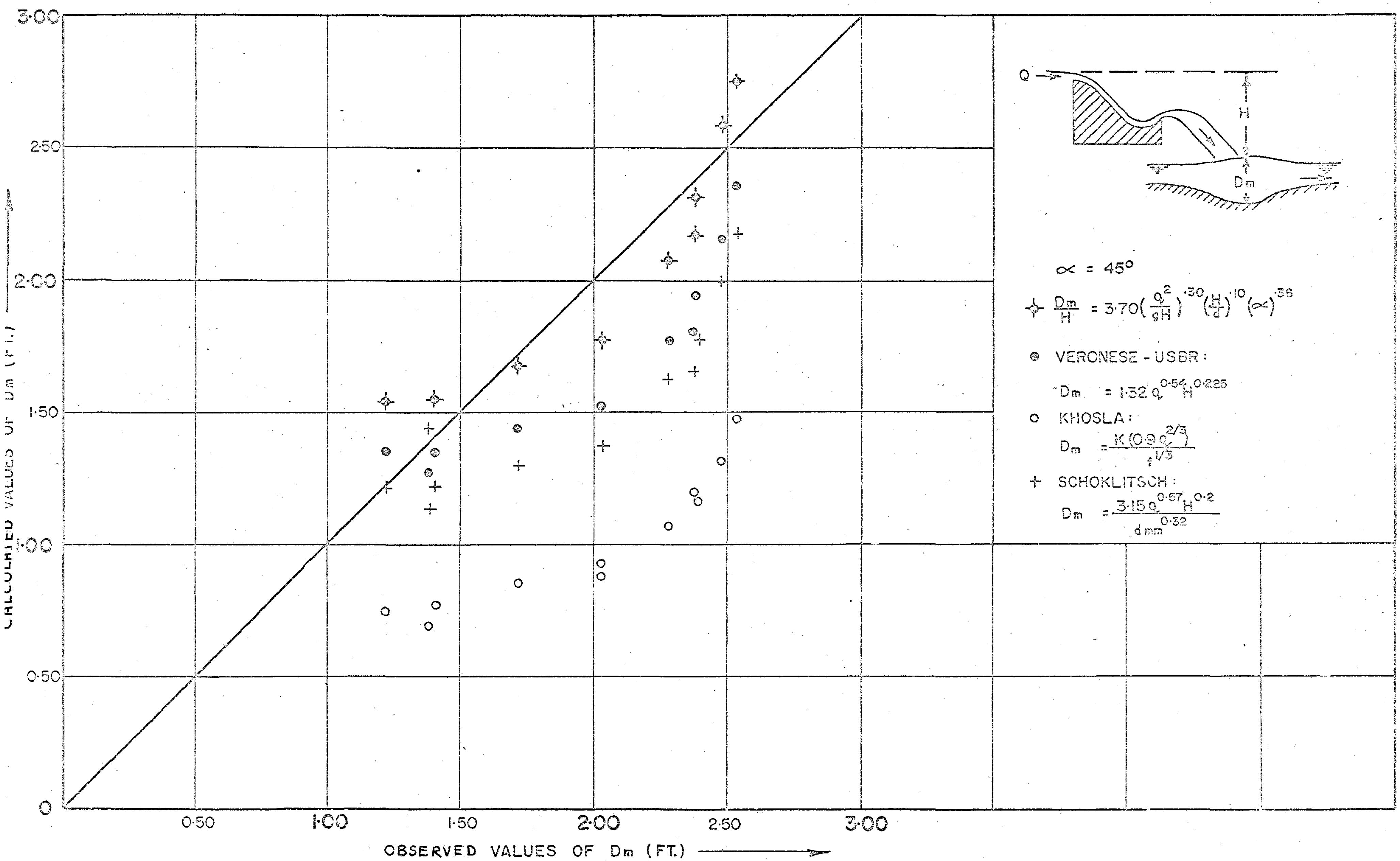

FIG. 19 OTHER EMPIRICAL EQUATIONS

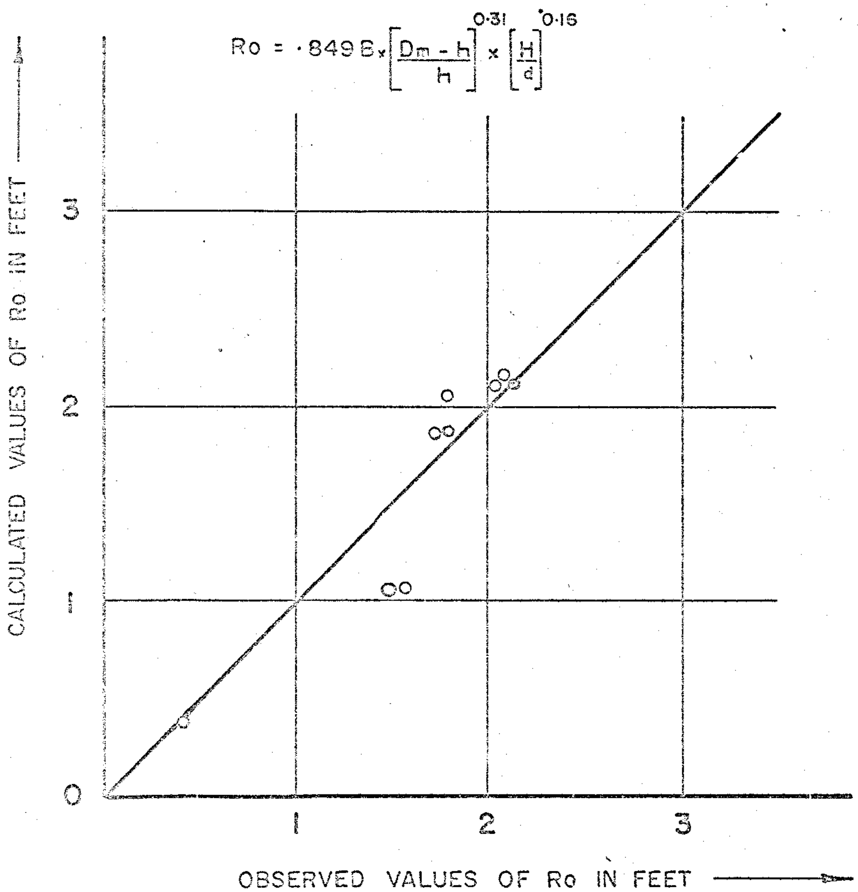
$R_o = \cdot 849\, B \times \left[\frac{D_m - h}{h}\right]^{0.31} \times \left[\frac{H}{d}\right]^{0.16}$
CALCULATED VALUES OF Ro IN FEET
OBSERVED VALUES OF Ro IN FEET
0
1
2
3

FIG. 19

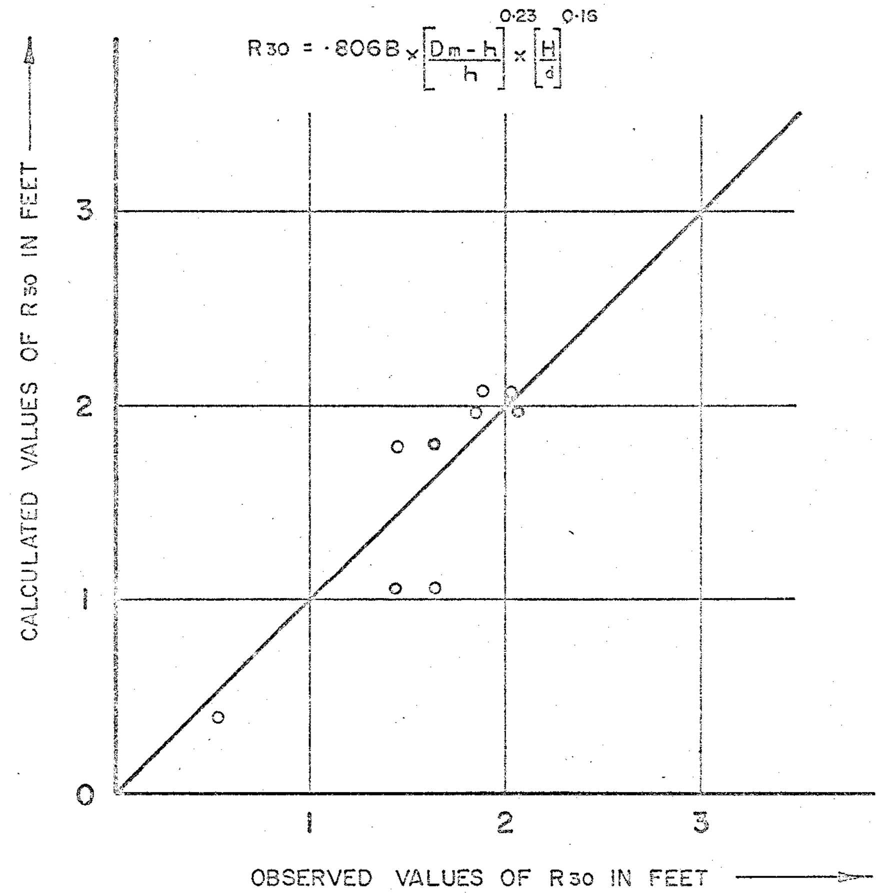
$R_{30} = \cdot 806\, B \times \left[\frac{D_m - h}{h}\right]^{0.23} \times \left[\frac{H}{d}\right]^{0.16}$
CALCULATED VALUES OF R30 IN FEET
OBSERVED VALUES OF R30 IN FEET
0
1
2
3

FIG. 20

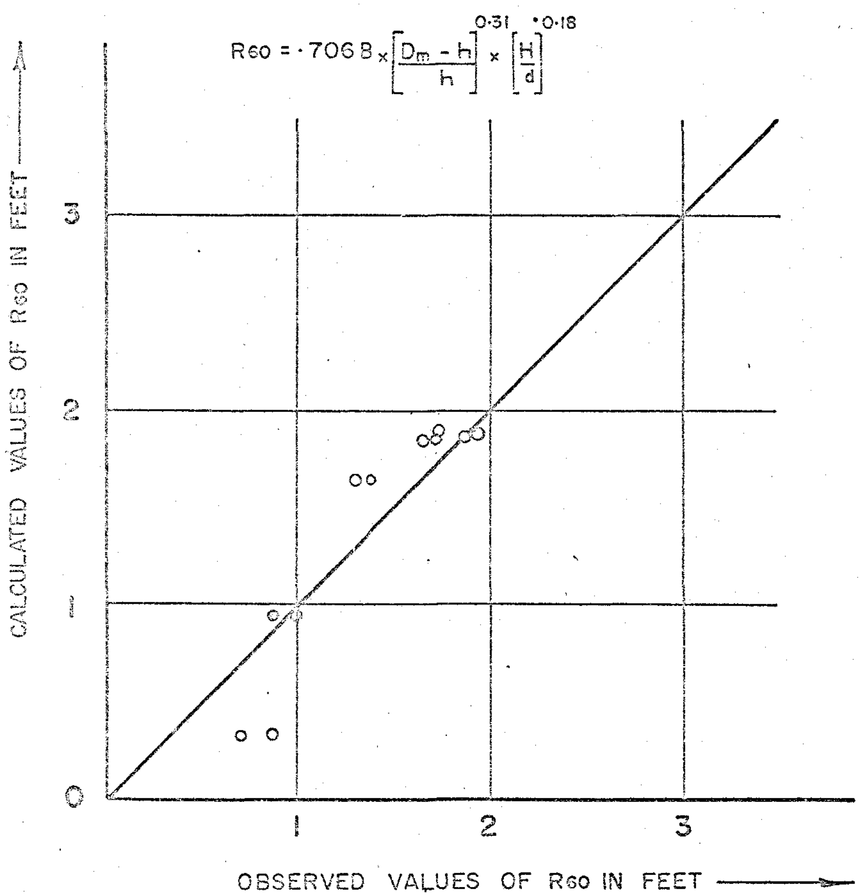
R60 = ·706 B × [(Dm - h)/h]^0.31 × [H/d]^0.18
CALCULATED VALUES OF R60 IN FEET
OBSERVED VALUES OF R60 IN FEET
0
1
2
3

FIG. 21

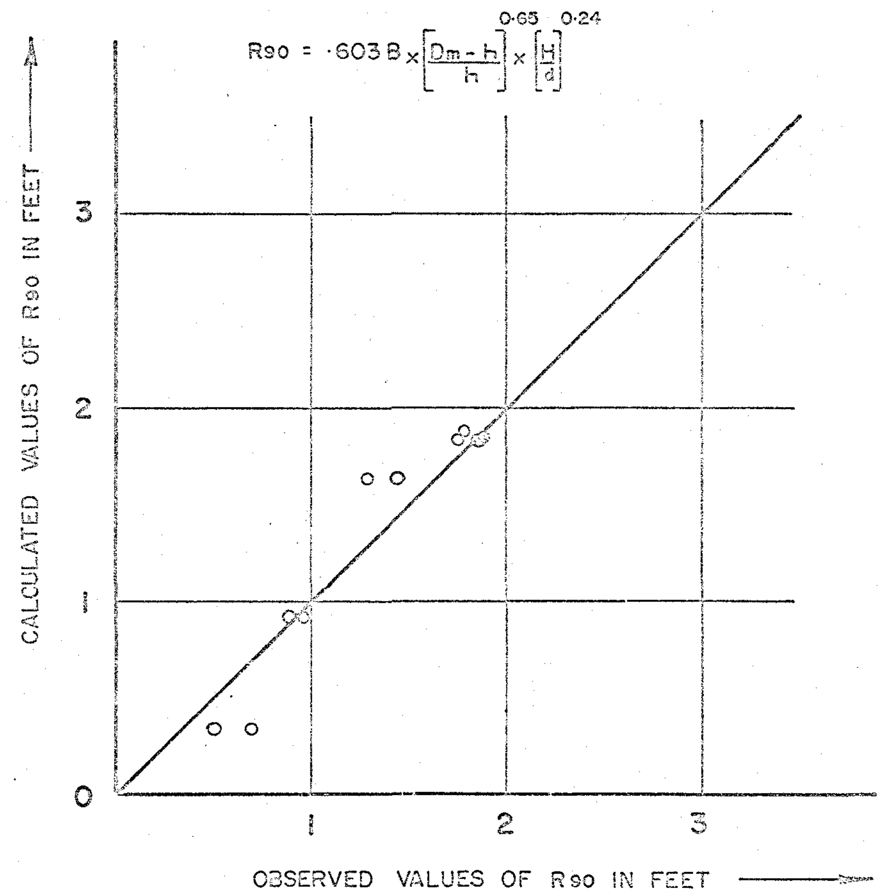
R90 = ·603 B × [(Dm - h)/h]^0.65 × [H/d]^0.24
CALCULATED VALUES OF R90 IN FEET
OBSERVED VALUES OF R90 IN FEET
0
1
2
3

FIG. 22

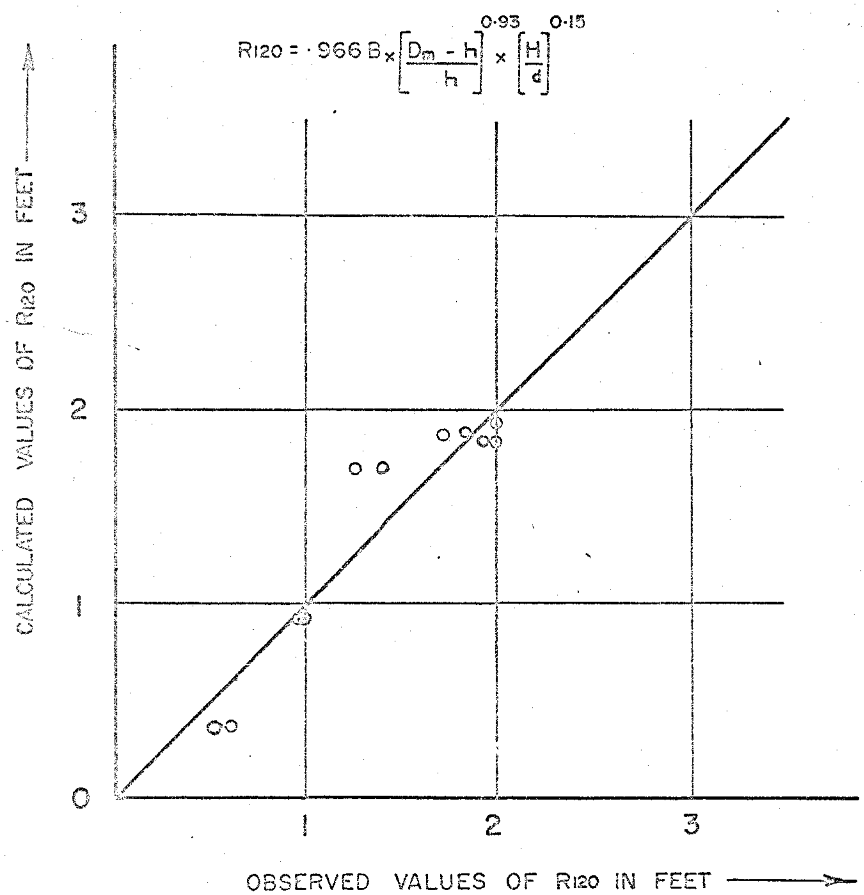
$R_{120} = \cdot 966\, B \times \left[\frac{D_m - h}{h}\right]^{0\cdot 93} \times \left[\frac{H}{d}\right]^{0\cdot 15}$
CALCULATED VALUES OF R120 IN FEET
OBSERVED VALUES OF R120 IN FEET
0
1
2
3

FIG. 23

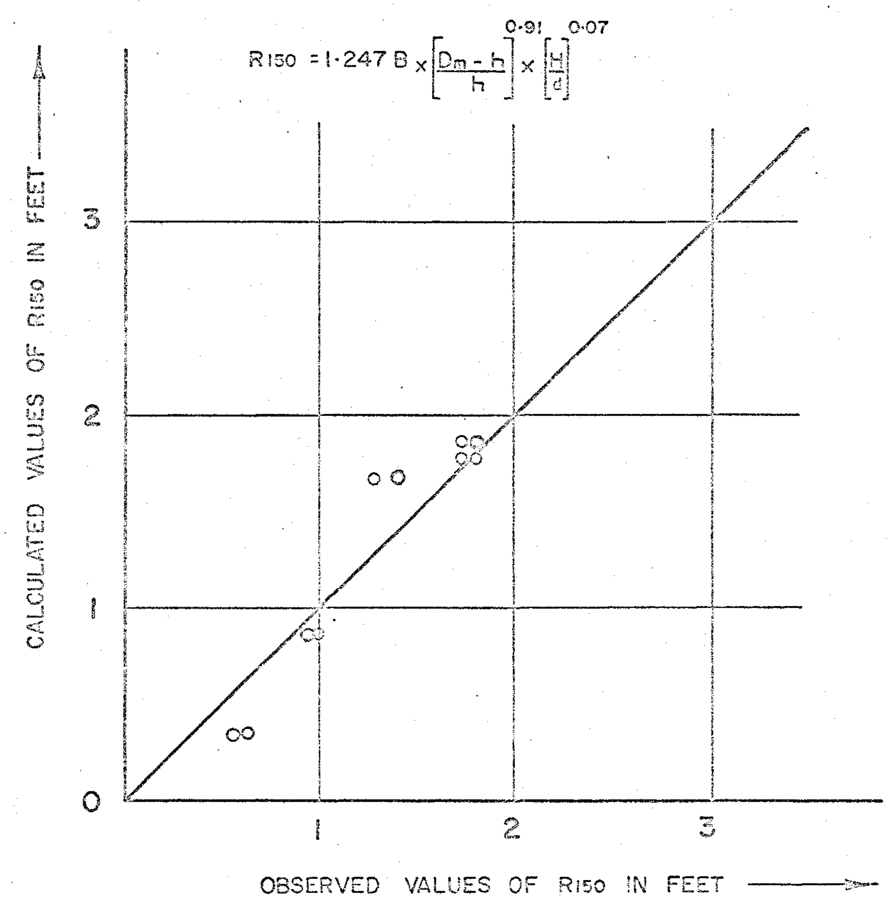
$R_{150} = 1\cdot 247\, B \times \left[\frac{D_m - h}{h}\right]^{0\cdot 91} \times \left[\frac{H}{d}\right]^{0\cdot 07}$
CALCULATED VALUES OF R150 IN FEET
OBSERVED VALUES OF R150 IN FEET
0
1
2
3

FIG. 24

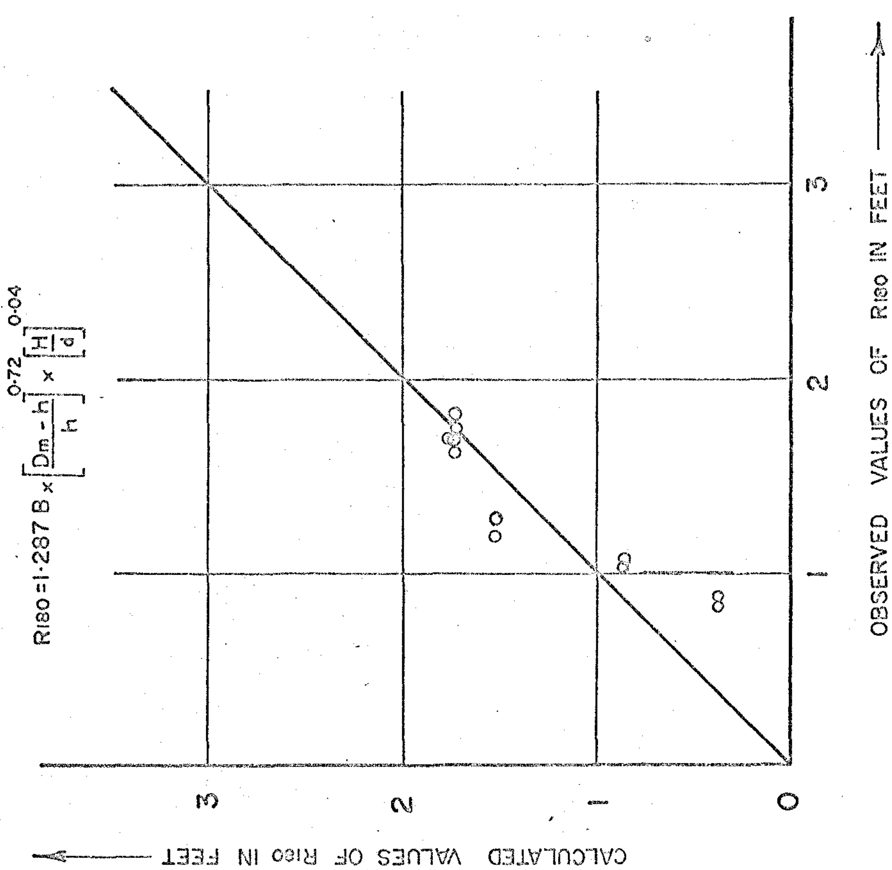

R180 = 1·287 B x [Dm - h / h]^0·72 x [H / d]^0·04
OBSERVED VALUES OF R180 IN FEET
CALCULATED VALUES OF R180 IN FEET
0
1
2
3
1
2
3

FIG. 25

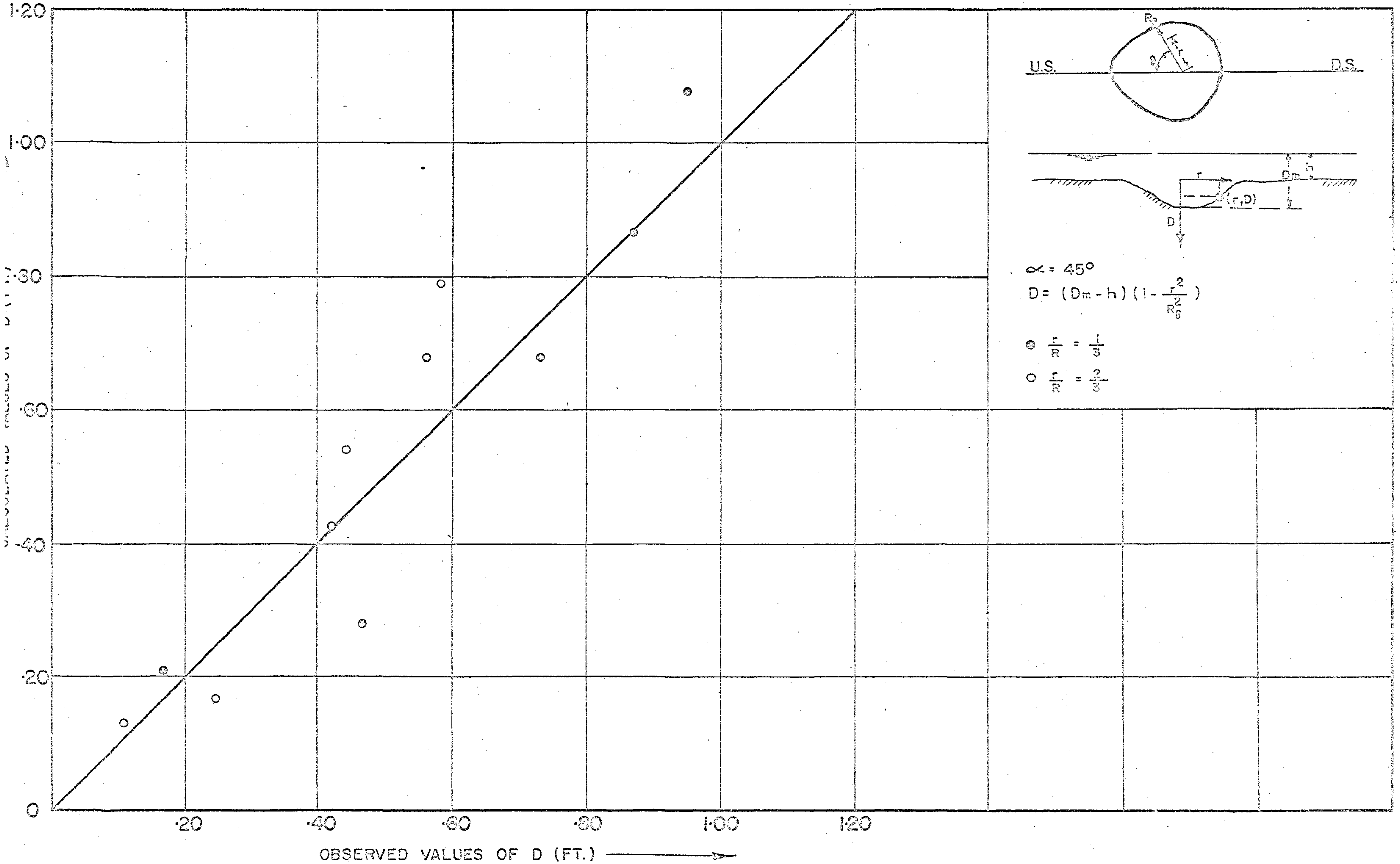
1·20
1·00
·80
·60
·40
·20
0
·20
·40
·60
·80
1·00
1·20
OBSERVED VALUES OF D (FT.)
U.S.
D.S.
(r,D)
∝ = 45°
D = (Dm - h)(1 - r²/R²)
r/R = 1/3
r/R = 2/3

FIG. 26

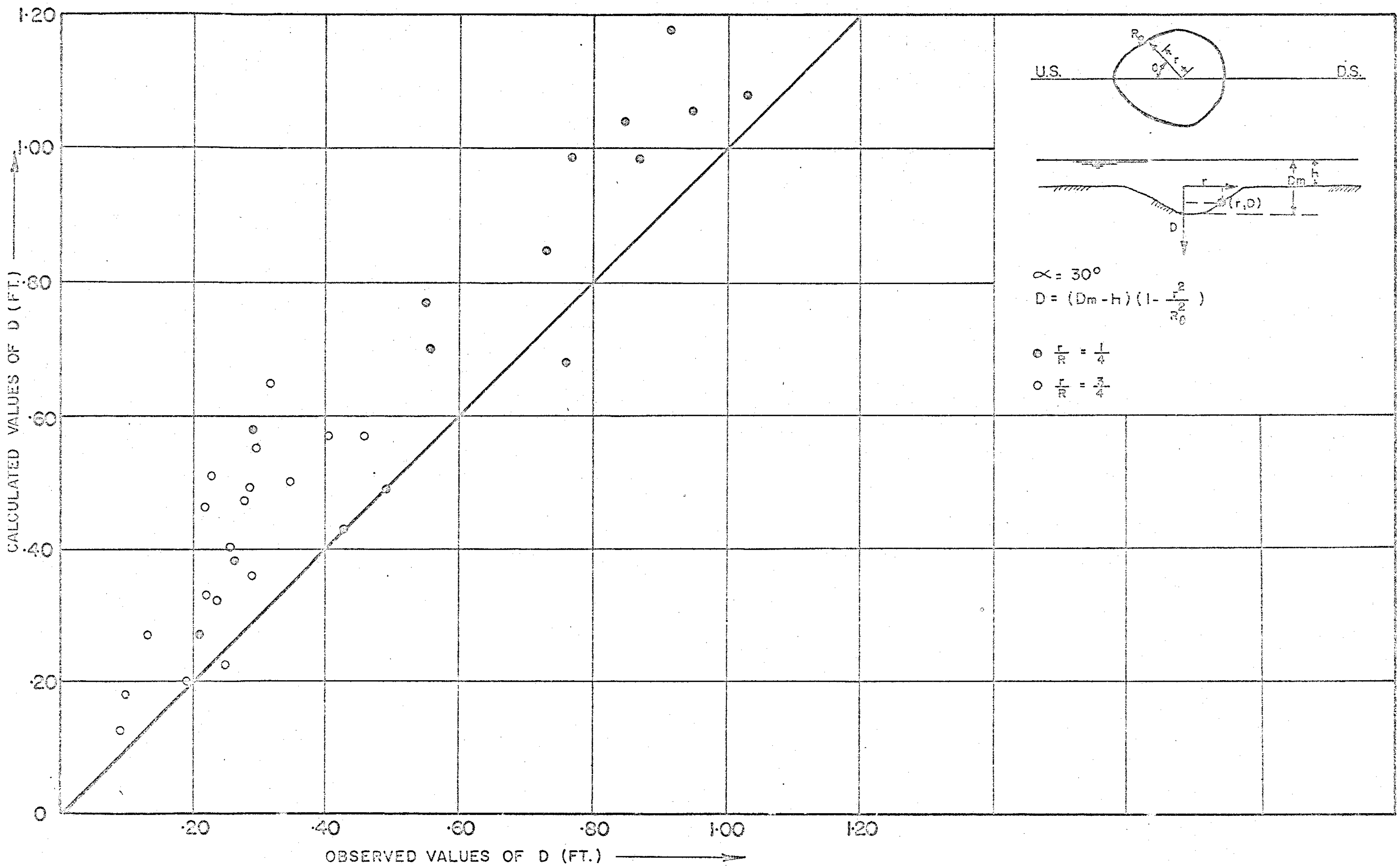
U.S.
D.S.
R_0
r
α
h
Dm
r
(r, D)
D
$\alpha = 30°$
$D = (Dm - h)(1 - \frac{r^2}{R_0^2})$
$\frac{r}{R} = \frac{1}{4}$
$\frac{r}{R} = \frac{3}{4}$
0
·20
·40
·60
·80
1·00
1·20
CALCULATED VALUES OF D (FT.)
OBSERVED VALUES OF D (FT.)

FIG. 27

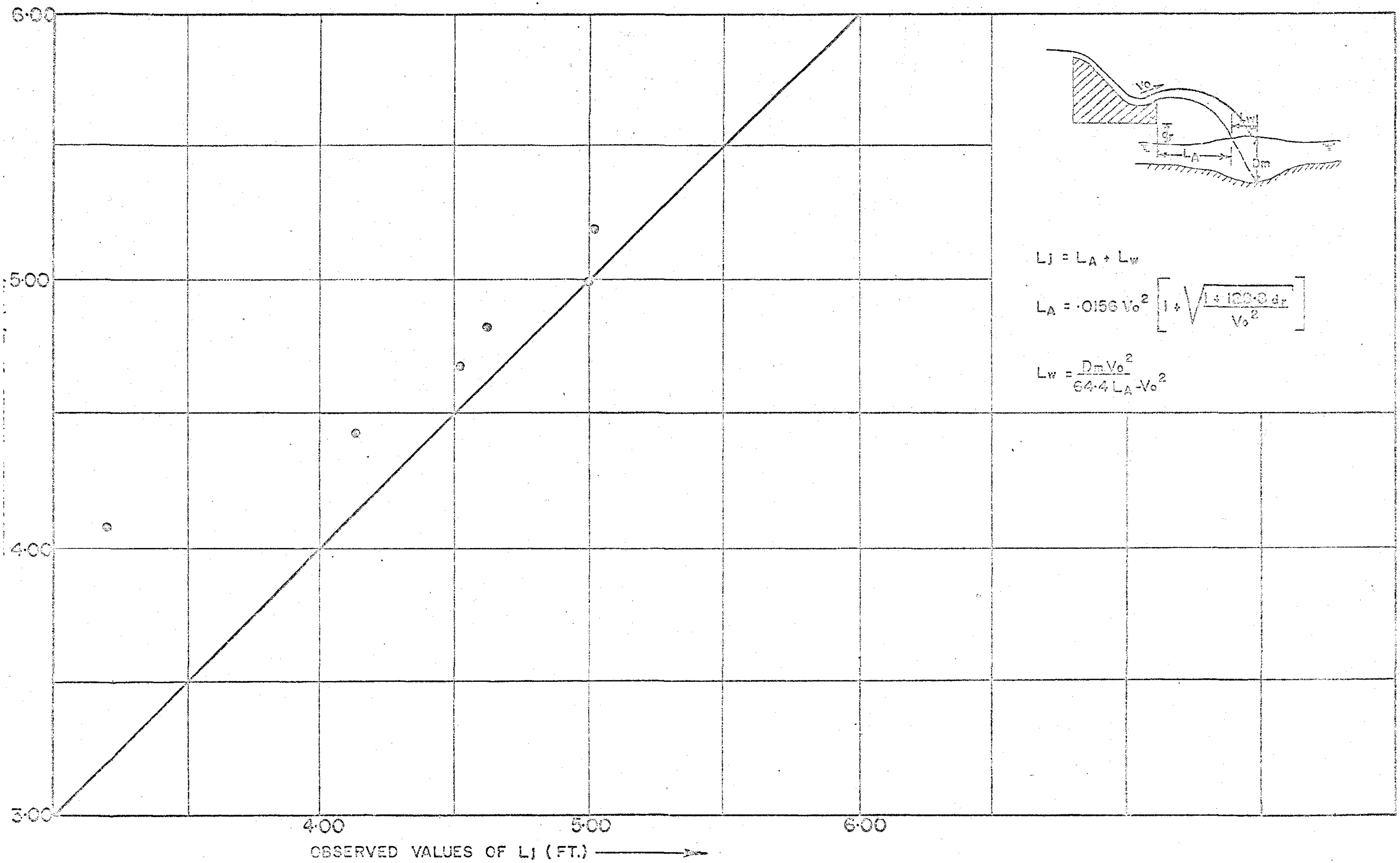

6·00
5·00
4·00
3·00
4·00
5·00
6·00
OBSERVED VALUES OF Lj (FT.)
$L_j = L_A + L_w$
$L_A = \cdot 0156\, V_o^2 \left[1 + \sqrt{\frac{1 + 128{\cdot}8\, d_r}{V_o^2}} \right]$
$L_w = \frac{D_m V_o^2}{64{\cdot}4\, L_A - V_o^2}$
Vo
Lw
dr
LA
Dm

FIG. 26

APPENDIX E.

Theoretical Scour Hole Configurations

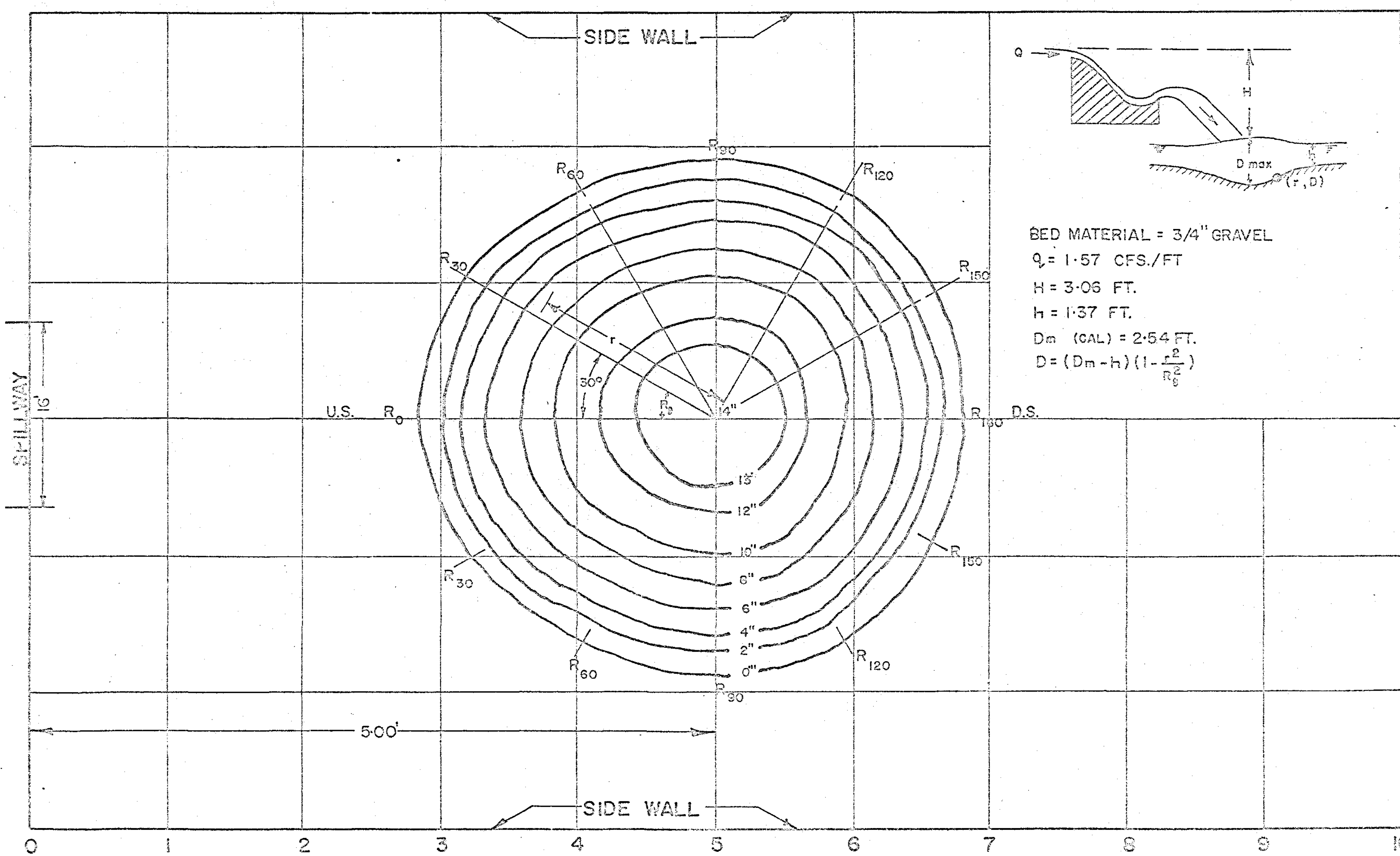

FIG.29 THEORETICAL SCOUR HOLE CONFIGURATION FOR $\alpha = 45°$

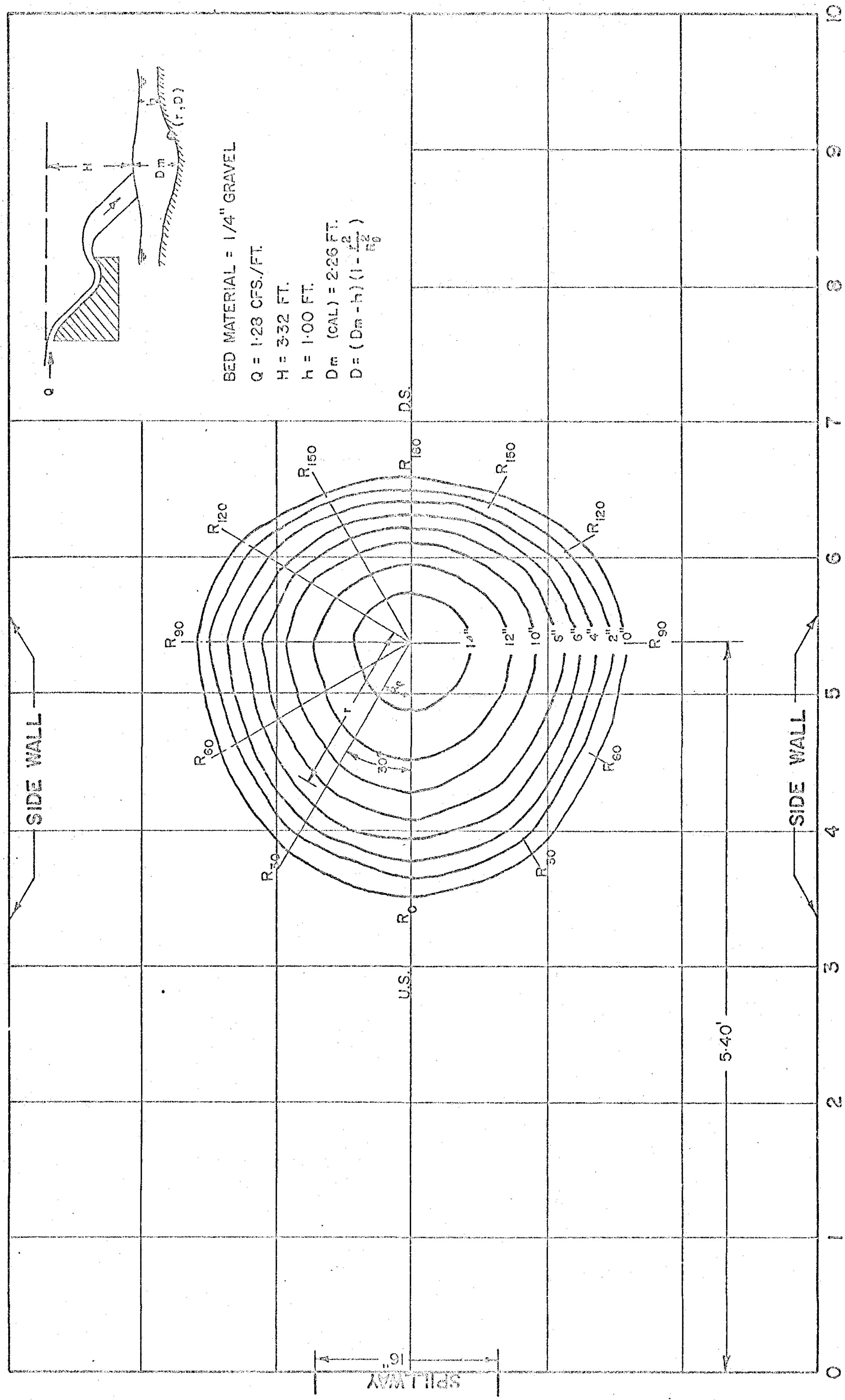

FIG. 30 THEORETICAL SCOUR HOLE CONFIGURATION FOR $\alpha = 30°$

$D = (D_m - h)\left(1 - \frac{r^2}{R_\theta^2}\right)$

APPENDIX F.

Theoretical Scour Hole Cross-sections

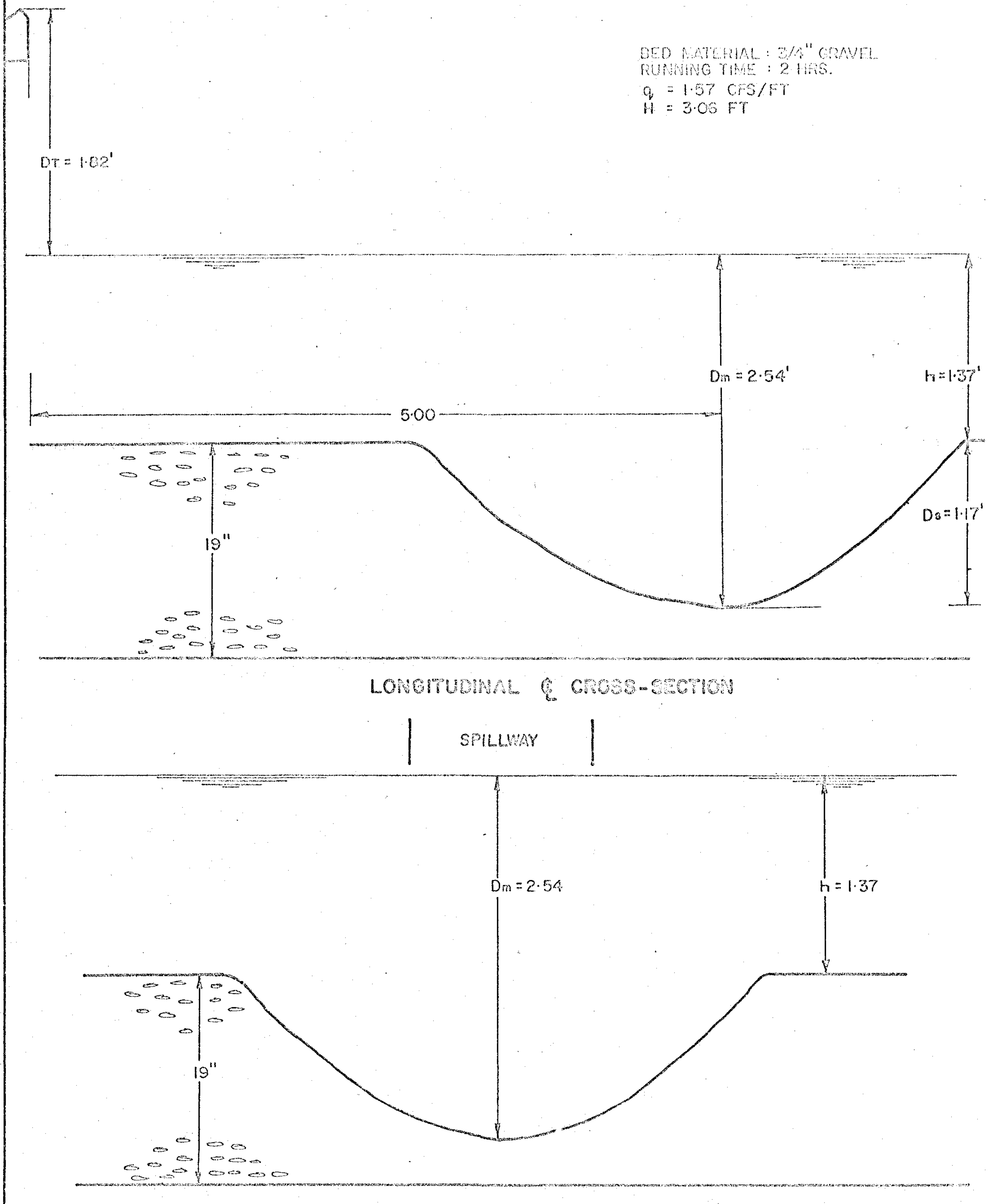

TRANSVERSE ℄ CROSS-SECTION

THEORITICAL SCOUR HOLE CONFIGURATION $\alpha = 45°$

FIG. 31

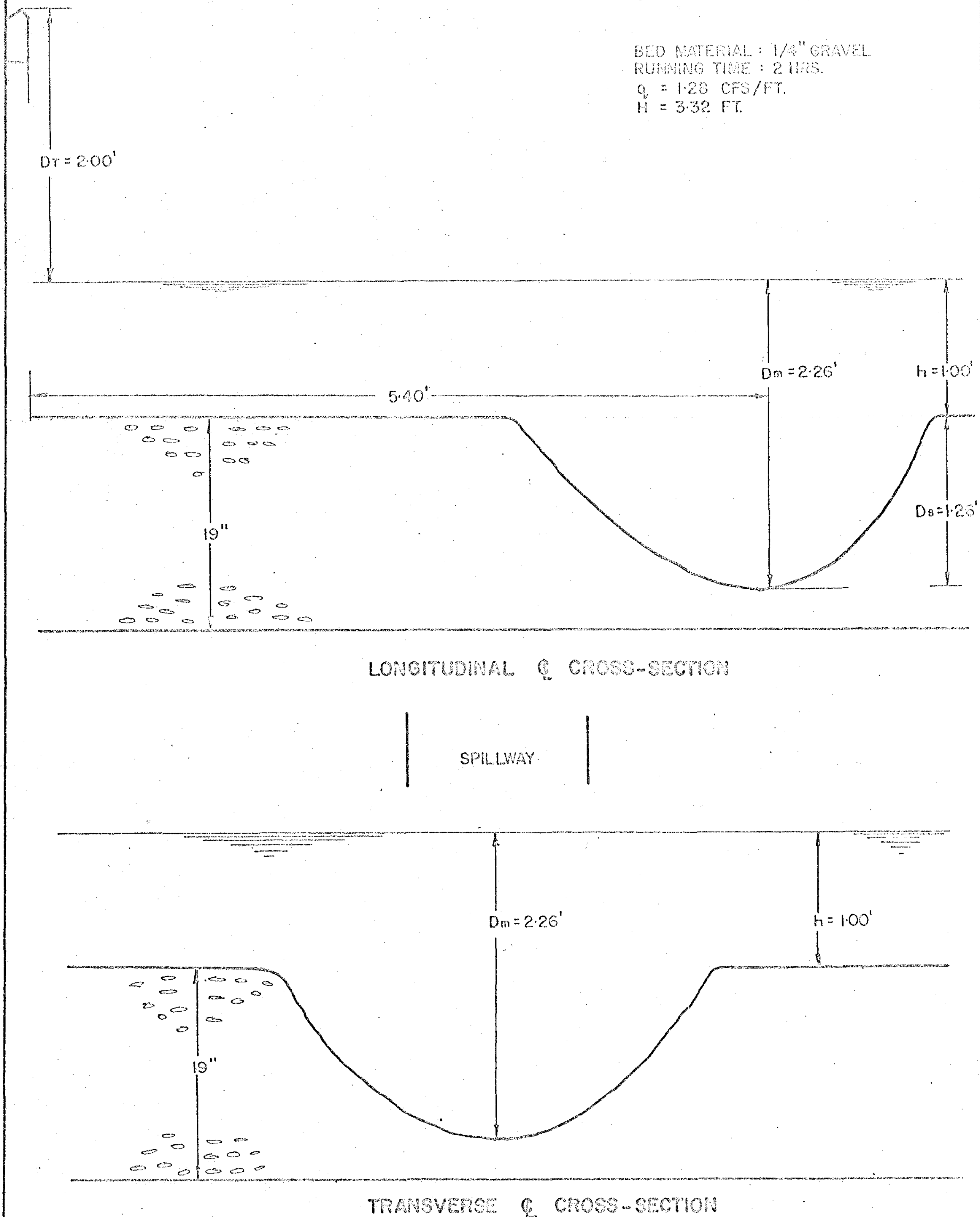

THEORITICAL SCOUR HOLE CONFIGURATION $\alpha = 30°$

FIG. 32

APPENDIX G.

Correlation Coefficients

LEGEND

r = CORRELATION COEFFICIENT

$Y = bo(X_1)^{b1}(X_2)^{b2}(X_3)^{b3}$

$A = LOG_eY - (LOG_eY)_{AVE}$

$B = LOG_eX_1 - (LOG_eX_1)_{AVE}$

$C = LOG_eX_2 - (LOG_eX_2)_{AVE}$

$D = LOG_eX_3 - (LOG_eX_3)_{AVE}$

rmc = multiple correlation coefficient $= \sqrt{\dfrac{b_1\sum AB + b_2\sum AC + b_3\sum AD}{\sum AA}}$

EQUATION	Y	X_1	X_2	X_3	r_{mc}	Min. Value of r at 5% level of Significance
$\frac{Dm}{H}=3.70\left(\frac{q^2}{gH^3}\right)^{.30}\left(\frac{H}{d}\right)^{.10}\left(\alpha\right)^{.36}$	$\frac{Dm}{H}$	$\frac{q^2}{gH^3}$	$\frac{H}{d}$	α	0.946	0.445
$\frac{Ro}{B}=0.85\left(\frac{Dm-h}{h}\right)^{.31}\left(\frac{H}{d}\right)^{.16}$	$\frac{Ro}{B}$	$\frac{Dm-h}{h}$	$\frac{H}{d}$		0.818	0.697
$\frac{R30}{B}=0.81\left(\frac{Dm-h}{h}\right)^{.23}\left(\frac{H}{d}\right)^{.16}$	$\frac{R30}{B}$	$\frac{Dm-h}{h}$	$\frac{H}{d}$		0.721	0.697
$\frac{R60}{B}=0.71\left(\frac{Dm-h}{h}\right)^{.31}\left(\frac{H}{d}\right)^{.18}$	$\frac{R60}{B}$	$\frac{Dm-h}{h}$	$\frac{H}{d}$		0.753	0.697
$\frac{R90}{B}=0.60\left(\frac{Dm-h}{h}\right)^{.65}\left(\frac{H}{d}\right)^{.24}$	$\frac{R90}{B}$	$\frac{Dm-h}{h}$	$\frac{H}{d}$		0.821	0.697
$\frac{R120}{B}=0.97\left(\frac{Dm-h}{h}\right)^{.93}\left(\frac{H}{d}\right)^{.15}$	$\frac{R120}{B}$	$\frac{Dm-h}{h}$	$\frac{H}{d}$		0.896	0.687
$\frac{R150}{B}=1.25\left(\frac{Dm-h}{h}\right)^{.91}\left(\frac{H}{d}\right)^{.07}$	$\frac{R150}{B}$	$\frac{Dm-h}{h}$	$\frac{H}{d}$		0.990	0.697
$\frac{R180}{B}=1.29\left(\frac{Dm-h}{h}\right)^{.72}\left(\frac{H}{d}\right)^{.04}$	$\frac{R180}{B}$	$\frac{Dm-h}{h}$	$\frac{H}{d}$		0.907	0.697

EQUATION	REMARKS	Y	X_1	X_2	r_{mc}	Min. Value of r at 5% level of Significance
$D = (D_m - h)\left(1 - \frac{r^2}{R_\theta^2}\right)$	$\frac{r}{R_\theta} = \frac{1}{3}$, $\alpha = 45°$	D	$D_m - h$	$1 - \frac{r^2}{R_\theta^2}$	0.978	0.378
$D = (D_m - h)\left(1 - \frac{r^2}{R_\theta^2}\right)$	$\frac{r}{R_\theta} = \frac{2}{3}$, $\alpha = 45°$	D	$D_m - h$	$1 - \frac{r^2}{R_\theta^2}$	0.882	0.378
$D = (D_m - h)\left(1 - \frac{r^2}{R_\theta^2}\right)$	$\frac{r}{R_\theta} = \frac{1}{4}$, $\alpha = 30°$	D	$D_m - h$	$1 - \frac{r^2}{R_\theta^2}$	0.759	0.218
$D = (D_m - h)\left(1 - \frac{r^2}{R_\theta^2}\right)$	$\frac{r}{R_\theta} = \frac{3}{4}$, $\alpha = 30°$	D	$D_m - h$	$1 - \frac{r^2}{R_\theta^2}$	0.646	0.218
$D = (D_m - h)\left(1 - \frac{r^2}{R_\theta^2}\right)$	$\frac{r}{R_\theta} = \frac{1}{3} - \frac{2}{3}$, $\alpha = 45°$	D	$D_m - h$	$1 - \frac{r^2}{R_\theta^2}$	0.499	0.270
$D = (D_m - h)\left(1 - \frac{r^2}{R_\theta^2}\right)$	$\frac{r}{R_\theta} = \frac{1}{4} - \frac{3}{4}$, $\alpha = 30°$	D	$D_m - h$	$1 - \frac{r^2}{R_\theta^2}$	0.780	0.156

APPENDIX H.

Tabulation of Experimental Results

TABLE No. 1

TYPE : WITH REMOVAL OF DEPOSITED MATERIAL

BED MATERIAL : 3/4" GRAVEL

SPILLWAY WIDTH : 16"

BUCKET RADIUS : 8"

FLIP BUCKET ANGLE : 45°

EXPT. No.	Q USGPM	q cfs/ft.	H ft.	h ft.	DEPTH OF SCOUR, D_m (ft.)		D_m/H	
					OBS.	CALC.	OBS.	CALC.
1	365	0.61	2.92	1.21	1.40	1.45	0.48	0.50
2	515	0.86	2.82	1.47	2.04	1.78	0.72	0.63
3	675	1.13	2.83	1.32	2.28	2.09	0.81	0.74
4	780	1.30	3.02	1.33	2.39	2.31	0.79	0.76
5	940	1.57	3.06	1.37	2.48	2.59	0.81	0.85
6	1100	1.84	3.05	1.43	2.54	2.85	0.83	0.93

TABLE No. 2

TYPE : NO SCOUR ALLOWED

BED MATERIAL : 3/4" GRAVEL

SPILLWAY WIDTH : 16"

BUCKET RADIUS : 8"

FLIP BUCKET ANGLE : 45

EXPT. No.	Q USGPM	q cfs/ft.	H ft.	h ft.	DEPTH OF SCOUR, D_m (ft.)		D_m/H	
					OBS.	CALC.	OBS.	CALC.
7	405	0.67	2.93	1.24	1.24	1.55	0.42	0.53
8	420	0.70	2.73	1.42	1.42	1.56	0.52	0.57
9	490	0.82	2.45	1.73	1.73	1.68	0.71	0.68
10	560	0.93	2.20	2.04	2.04	1.78	0.93	0.81
11	810	1.35	1.96	2.37	2.37	2.17	1.21	1.11

TABLE No. 3

$\alpha = 30°$; DATA FROM THE RESULTS OF PADIYAR (5)

$$\frac{D_m}{H} = 3.695 \left(\frac{q^2}{gH^3}\right)^{.30} \left(\frac{H}{d}\right)^{.28} \alpha^{.36} \qquad D_m = 1.301 \frac{q^{.60} H^{.20} \alpha^{.36}}{d^{.10}}$$

EXPT. No.	B in.	R_B in.	BED Material (CR.)	Q USGPM	q cfs/ft	H ft.	h in.	Depth of Scour D_m(ft)		D_m/H	
								OBS.	CALC.	OBS.	CALC.
1a	24	12	1/4"	250	0.28	2.93	4.50	0.88	0.89	0.30	0.31
2a	24	12	1/4"	360	0.40	2.96	4.50	1.02	1.11	0.34	0.38
3a	24	12	1/4"	450	0.50	2.98	5.38	1.24	1.27	0.42	0.43
4a	24	12	1/4"	650	0.73	2.97	6.38	1.54	1.58	0.52	0.53
5a	24	12	1/4"	1050	1.18	2.81	9.50	2.19	2.09	0.77	0.74
6a	24	12	3/4"	250	0.28	2.75	6.00	0.77	0.79	0.28	0.29
7a	24	12	3/4"	500	0.56	2.65	9.25	1.27	1.18	0.48	0.45
8a	24	12	3/4"	750	0.84	2.42	12.25	1.61	1.48	0.67	0.61
9a	24	12	3/4"	1000	1.13	2.92	8.00	2.01	1.82	0.69	0.62
10a	24	12	3/4"	1250	1.41	2.88	9.50	2.27	2.02	0.79	0.72
11a	16	8	1/4"	350	0.59	3.46	7.50	1.65	1.44	0.48	0.42
12a	16	8	1/4"	500	0.85	3.40	9.38	2.00	1.89	0.59	0.56
13a	16	8	1/4"	750	1.27	3.32	12.00	2.23	2.25	0.67	0.68

CONTINUED

14a	16	8	1/4"	1000	1.70	3.22	14.13	2.42	2.65	0.76	0.83
15a	16	8	3/4"	250	0.42	3.38	5.88	0.86	1.11	0.26	0.33
16a	16	8	3/4"	500	0.85	3.25	9.25	1.86	1.68	0.57	0.51
17a	16	8	3/4"	750	1.27	3.21	11.25	2.08	2.00	0.65	0.62
18a	16	8	3/4"	1000	1.70	3.08	13.50	2.29	2.34	0.74	0.76
19a	24	12	1/4"	450	0.51	2.98	14.00	1.17	1.27	0.39	0.43
20a	24	12	1/4"	190	0.21	2.90	8.25	0.69	0.75	0.24	0.26
21a	24	12	1/4"	265	0.30	2.93	10.50	0.88	0.92	0.30	0.31
22a	24	12	1/4"	370	0.38	2.96	12.25	1.02	1.08	0.34	0.36
23a	24	12	1/4"	650	0.73	2.97	17.38	1.45	1.58	0.49	0.53
24a	16	8	1/4"	350	0.59	3.45	7.75	1.65	1.44	0.48	0.42
25a	16	8	1/4"	210	0.33	3.48	5.88	1.06	1.02	0.30	0.29
26a	16	8	1/4"	500	0.85	3.40	9.38	2.00	1.77	0.59	0.52
27a	16	8	1/4"	750	1.28	3.33	12.00	2.23	2.26	0.67	0.68
28a	16	8	1/4"	1000	1.71	3.22	14.13	2.42	2.67	0.75	0.83

TABLE No. 4

MAXIMUM DEPTH OF SCOUR CALCULATED FROM

EQUATIONS DEVELOPED BY VERONESE-U.S.B.R., KHOSLA AND SCHOKLITSCH

$\alpha = 45°$ d = .0625'

EXPT. No.	Q USGPM	q cfs/ft	H ft.	h ft.	OBSERVED DEPTH OF SCOUR ft.	CALCULATED DEPTH OF SCOUR (ft.)		
						VERONESE	KHOSLA	SCHOKLITSCH
1	365	0.61	2.92	1.21	1.40	1.29	0.71	1.15
2	515	0.86	2.82	1.47	2.04	1.54	0.90	1.39
3	675	1.13	2.83	1.32	2.28	1.78	1.08	1.64
4	780	1.30	3.02	1.33	2.39	1.95	1.18	1.79
5	940	1.57	3.06	1.37	2.48	2.16	1.34	2.00
6	1100	1.84	3.05	1.43	2.54	2.36	1.49	2.18
7	405	0.67	2.93	1.24	1.24	1.37	0.77	1.23
8	420	0.70	2.73	1.42	1.42	1.37	0.79	1.23
9	490	0.82	2.45	1.73	1.73	1.45	0.87	1.31
10	560	0.93	2.20	2.04	2.04	1.52	0.95	1.39
11	810	1.35	1.96	2.37	2.37	1.81	1.22	1.67

VERONESE-USBR

$$D_m = 1.32\, q^{0.54}\, H^{0.225}$$

KHOSLA

$$D_m = \frac{K(0.9q^{2/3})}{f^{1/3}}; \quad f = 8d_{in}^{1/2} \text{ (Lacey silt factor);}$$

K(empirical coef.) assumed = 2.1

SHODLITSCH

$$D = \frac{3.15\, q^{0.57}\, H^{0.2}}{d_{mm}^{0.32}}$$

TABLE No. 5

DATA AND CALCULATED VALUES OF RADIUS VECTORS

$B = 16''$ BUCKET RADIUS $= 8''$ $\alpha = 45°$

EXPT. No.	OBSERVED VALUES IN FT.							CALCULATED VALUES IN FT.						
	R_0	R_{30}	R_{60}	R_{90}	R_{120}	R_{150}	R_{180}	R_0	R_{30}	R_{60}	R_{90}	R_{120}	R_{150}	R_{180}
1	0.40	0.52	0.83	0.67	0.60	0.63	0.86	0.37	0.36	0.34	0.34	0.36	0.35	0.33
2	1.58	1.63	0.96	0.94	0.94	1.00	1.08	1.05	1.03	0.94	0.90	0.91	0.86	0.86
3	1.71	1.45	1.29	1.26	1.27	1.25	1.19	1.84	1.78	1.65	1.63	1.59	1.62	1.57
4	1.77	1.83	1.64	1.73	1.71	1.73	1.60	2.04	1.98	1.84	1.82	1.87	1.78	1.73
5	2.08	2.02	1.71	1.77	2.00	1.73	1.69	2.12	2.06	1.90	1.87	1.91	1.82	1.78
6	2.03	1.89	1.88	1.83	2.00	1.77	1.75	2.09	2.04	1.88	1.82	1.83	1.75	1.71

$$0°: R_0 = .849\,B\left[\frac{D_m-h}{h}\right]^{0.31}\left[\frac{H}{d}\right]^{0.16}$$

$$30°: R_{30} = .806\,B\left[\frac{D_m-h}{h}\right]^{0.23}\left[\frac{H}{d}\right]^{0.16}$$

$$60°: R_{60} = .706\,B\left[\frac{D_m-h}{h}\right]^{0.31}\left[\frac{H}{d}\right]^{0.18}$$

$$90°: R_{90} = .603\,B\left[\frac{D_m-h}{h}\right]^{0.65}\left[\frac{H}{d}\right]^{0.24}$$

$$120°: R_{120} = .966\,B\left[\frac{D_m-h}{h}\right]^{0.93}\left[\frac{H}{d}\right]^{0.15}$$

$$150°: R_{150} = 1.247\,B\left[\frac{D_m-h}{h}\right]^{0.91}\left[\frac{H}{d}\right]^{0.07}$$

$$180°: R_{180} = 1.287\,B\left[\frac{D_m-h}{h}\right]^{0.72}\left[\frac{H}{d}\right]^{0.04}$$

TABLE No. 6

OBSERVED AND CALCULATED VALUES OF 'D' FOR r/R = 1/3

$\alpha = 45°$ B = 16" $R_B = 8"$ d = .0625'

EXPT. No.	OBSERVED VALUES OF 'D' (ft.)								$D_{cal.}$ (ft.)
	0°	30°	60°	90°	120°	150°	180°	AVE.	
1	0.17	0.17	0.17	0.17	0.17	0.17	0.16	0.17	0.21
2	0.45	0.45	0.48	0.46	0.47	0.50	0.50	0.47	0.28
3	0.85	0.83	0.75	0.67	0.58	0.74	0.79	0.74	0.68
4	0.93	0.98	0.94	0.79	0.79	0.81	0.90	0.88	0.87
5	1.04	1.03	1.01	0.91	0.78	0.92	1.00	0.96	1.08
6	1.02	1.03	0.93	0.84	0.78	0.97	1.04	0.94	1.26

TABLE No. 7

OBSERVED AND CALCULATED VALUES OF 'D' FOR r/R = 2/3

$\alpha = 45°$ B = 16" $R_B = 8"$ d = .0625'

EXPT. No.	OBSERVED VALUES OF 'D' (ft.)								$D_{cal.}$ (ft.)
	0°	30°	60°	90°	120°	150°	180°	AVE.	
1	0.14	0.14	0.11	0.11	0.10	0.11	0.07	0.11	0.13
2	0.13	0.07	0.38	0.32	0.25	0.29	0.33	0.25	0.17
3	0.58	0.50	0.46	0.38	0.29	0.29	0.50	0.43	0.43
4	0.50	0.50	0.50	0.45	0.39	0.40	0.38	0.45	0.54
5	0.74	0.71	0.75	0.54	0.31	0.42	0.54	0.57	0.68
6	0.64	0.75	0.67	0.55	0.39	0.46	0.67	0.59	0.79

$$D = (D_m - h)\left(1 - \frac{r^2}{R^2}\right) \quad ; \quad D_m = 1.301\,\frac{Q^{.60}\,H^{.20}\,\alpha^{.36}}{d^{.10}}$$

$$R = CB\left(\frac{D_m - h}{h}\right)^x \left(\frac{H}{d}\right)^y$$

TABLE No. 8

OBSERVED AND CALCULATED VALUES OF 'D' FOR $r/R_\phi = 1/4$

$\alpha = 30^\circ$

$D_m = (D_m - h)\left(1 - \frac{r^2}{R_\phi^2}\right)$ $\quad D_m = 1.301\, \frac{q^{.60} H^{.20} \alpha^{.36}}{d^{.10}}$ $\quad R_\phi = CB\left(\frac{D_m - h}{h}\right)^x \left(\frac{H}{d}\right)^y$

EXP. No.	B in.	R_B in.	Bed mat. GR.	OBSERVED VALUES OF D_{TW} (in.) 0°	30°	60°	90°	120°	150°	180°	AVE.	h IN.	D_{AVE} ft.	D_{CAL} ft.
1a	24	12	1/4"	9.38	10.38	10.63	10.38	10.38	10.63	10.63	10.34	4.50	0.49	0.49
2a	24	12	1/4"	9.50	11.50	11.50	11.50	11.50	11.00	11.00	11.21	4.50	0.56	0.70
3a	24	12	1/4"	12.88	12.38	13.38	13.88	13.88	12.88	12.88	13.23	5.38	0.55	0.77
4a	24	12	1/4"	16.38	16.13	16.13	16.38	15.88	15.38	15.38	15.95	6.38	0.77	0.99
5a	24	12	1/4"	25.25	24.25	23.25	22.25	22.25	24.25	24.25	23.68	9.50	1.19	1.22
6a	24	12	3/4"	8.25	8.25	8.50	8.50	8.75	8.75	8.50	8.50	6.00	0.21	0.27
7a	24	12	3/4"	12.50	12.25	12.50	12.25	12.25	12.25	12.75	12.39	9.25	0.26	0.38
8a	24	12	3/4"	17.25	17.25	17.25	17.25	17.25	17.25	18.25	17.39	12.25	0.43	0.43
9a	24	12	3/4"	20.50	20.50	20.50	20.25	20.00	20.00	21.25	20.40	8.00	1.03	1.08
10a	24	12	3/4"	24.25	24.50	24.00	22.25	22.50	23.00	25.25	23.25	9.50	1.15	1.21
11a	16	8	1/4"	16.25	16.75	16.75	16.25	16.25	16.75	16.75	16.54	7.50	0.76	0.68
12a	16	8	1/4"	21.38	20.88	19.88	19.38	18.88	18.88	17.88	19.58	9.38	0.85	1.04
13a	16	8	1/4"	24.00	24.00	23.00	22.75	22.25	22.50	23.00	23.07	12.00	0.92	1.18
14a	16	8	1/4"	26.63	26.63	26.13	24.13	24.13	25.63	26.38	25.67	14.13	0.96	1.38
15a	16	8	3/4"	9.38	9.38	9.38	9.38	9.38	9.38	9.38	9.38	5.88	0.29	0.53
16a	16	8	3/4"	19.25	18.75	19.25	19.25	18.75	18.25	17.50	18.00	9.25	0.73	0.85
17a	16	8	3/4"	22.25	22.25	22.25	21.25	21.25	21.25	21.25	21.68	11.25	0.87	0.99
18a	16	8	3/4"	26.50	26.50	26.50	25.50	24.50	25.50	26.00	25.86	14.50	0.95	1.06

TABLE No. 9

OBSERVED AND CALCULATED VALUES OF 'D' FOR $r/R_\theta = 3/4$

$\alpha = 30°$

$$D = (D_m - h)\left(1 - \frac{r^2}{R_\theta^2}\right) \qquad D_m = 1.301\,\frac{q^{.60} H^{.20} \alpha^{.36}}{d^{.10}} \qquad R_\theta = CB\left(\frac{D_m - h}{h}\right)^x \left(\frac{H}{d}\right)^y$$

EXP. No.	B in.	R_B in.	Bed mat. GR.	OBSERVED VALUES OF D_{TW} (in.) 0°	30°	60°	90°	120°	150°	180°	AVE.	h in.	D_{AVE} ft.	D_{CAL} ft.
1a	24	12	1/4"	6.38	7.88	9.13	7.38	7.38	6.88	6.88	7.42	4.50	0.25	0.23
2a	24	12	1/4"	7.50	7.50	6.50	7.00	7.50	6.75	6.75	7.07	4.50	0.22	0.33
3a	24	12	1/4"	6.13	9.38	8.38	8.38	9.88	9.38	9.38	8.84	5.38	0.29	0.36
4a	24	12	1/4"	8.63	7.88	9.38	8.88	9.38	9.38	9.38	8.99	6.38	0.22	0.46
5a	24	12	1/4"	14.75	17.00	15.75	15.25	15.25	13.75	13.75	15.07	9.50	0.46	0.57
6a	24	12	3/4"	6.50	6.50	7.06	7.00	7.75	7.50	7.75	7.14	6.00	0.09	0.13
7a	24	12	3/4"	11.00	10.25	11.25	10.25	10.25	10.25	10.75	10.43	9.25	0.10	0.18
8a	24	12	3/4"	14.25	14.25	14.50	14.50	14.50	14.75	14.25	14.57	12.25	0.19	0.20
9a	24	12	3/4"	11.75	12.00	12.00	12.00	12.00	11.00	11.75	11.79	8.00	0.23	0.51
10a	24	12	3/4"	15.75	16.50	13.50	13.50	12.25	13.30	16.50	14.47	9.50	0.41	0.57
11a	16	8	1/4"	8.25	9.75	11.75	9.75	10.25	10.75	11.50	10.29	7.50	0.24	0.32
12a	16	8	1/4"	14.88	14.38	13.88	12.38	11.88	11.88	11.38	12.81	9.38	0.29	0.49
13a	16	8	1/4"	16.00	17.00	16.00	14.75	14.50	16.00	15.00	15.61	12.00	0.30	0.55
14a	16	8	1/4"	19.13	19.13	18.13	17.13	16.88	17.13	18.83	18.02	14.13	0.32	0.65
15a	16	8	3/4"	6.88	7.63	7.88	7.88	7.63	6.88	7.38	7.45	5.88	0.13	0.27
16a	16	8	3/4"	11.25	10.75	13.25	13.25	13.25	12.25	12.25	12.32	9.25	0.26	0.40
17a	16	8	3/4"	15.25	16.25	15.25	15.25	14.25	13.25	13.25	14.68	11.25	0.28	0.47
18a	16	8	3/4"	20.50	18.50	20.50	18.00	17.50	17.50	18.50	18.79	14.50	0.35	0.50

TABLE No. 10

DATA FOR CALCULATION OF JET TRAJECTORY LENGTH

FLIP BUCKET ANGLE : 45°

$$L_j = L_A + L_W$$

$$L_A = .0156\, V_o^2 \left[1 + \sqrt{\frac{1 + 128.8 d_T}{V_o^2}} \right] \; ; \; L_W = \frac{D_m V_o^2}{64.4 L_A - V_o^2}$$

EXPT. No.	q cfs/ft.	D_m ft.	V_o ft/sec.	d_T ft.	L_A ft.	L_W ft.	L_j ft.	$L_{obs.}$ ft.
1	0.61	1.40	8.34	1.97	3.42	0.65	4.07	3.22
2	0.86	2.04	8.60	1.73	3.42	1.01	4.43	4.13
3	1.13	2.28	8.69	1.87	3.56	1.11	4.67	4.51
4	1.30	2.39	8.90	1.84	3.64	1.19	4.83	4.61
5	1.57	2.48	8.96	1.82	3.72	1.25	4.99	5.00
6	1.84	2.54	9.20	1.76	3.85	1.32	5.17	5.00

TABLE No. 11

TYPICAL SCOUR HOLE DATA FOR $\alpha = 45°$

q= 1.57 cfs/ft; H= 3.06 ft.; h= 1.37 ft.; BED MATERIAL : 3/4" GR; B= 16"

D_m(cal.) = 2.54 ft.

θ (deg.)	R_θ (cal.) (ft.)	CALCULATED VALUES OF 'r' (ft.)							
		D=0"	D=2"	D=4"	D=6"	D=8"	D=10"	D=12"	D=13"
0	2.12	2.12	1.95	1.80	1.61	1.38	1.14	0.81	0.59
30	2.06	2.06	1.90	1.75	1.57	1.34	1.11	0.78	0.58
60	1.90	1.90	1.75	1.62	1.44	1.24	1.03	0.72	0.53
90	1.87	1.87	1.72	1.59	1.42	1.22	1.01	0.71	0.52
120	1.91	1.91	1.76	1.62	1.45	1.24	1.03	0.73	0.53
150	1.82	1.82	1.67	1.55	1.38	1.18	0.98	0.69	0.51
180	1.78	1.78	1.64	1.51	1.35	1.16	0.96	0.68	0.50

TABLE No. 12

TYPICAL SCOUR HOLE DATA FOR $\alpha = 30°$

q= 1.28cfs/ft; H=3.32 ft.; h=1.00 ft.; BED MATERIAL : 1/4" GR.; B=16"

D_m(cal.) = 2.26 ft.

θ (deg.)	R_θ (cal.) (ft.)	CALCULATED VALUES OF 'r' (ft.)							
		D=0"	D=2"	D=4"	D=6"	D=8"	D=10"	D=12"	D=14"
0	1.88	1.88	1.75	1.62	1.47	1.30	1.09	0.86	0.51
30	1.81	1.81	1.68	1.56	1.41	1.25	1.05	0.83	0.49
60	1.61	1.61	1.50	1.38	1.26	1.11	0.93	0.74	0.43
90	1.59	1.59	1.48	1.37	1.24	1.10	0.92	0.73	0.43
120	1.44	1.44	1.34	1.24	1.12	0.99	0.84	0.66	0.39
150	1.27	1.27	1.18	1.09	0.99	0.88	0.74	0.58	0.34
180	1.22	1.22	1.13	1.05	0.95	0.84	0.71	0.56	0.33

$$D = (D_m - h)\left(1 - \frac{r^2}{R_\theta^2}\right) \qquad r = R_\theta \sqrt{\frac{D_m - h - D}{D_m - h}}$$

BIBLIOGRAPHY

1. Veronese-USBR, Design of Small Dams, U.S.B.R., 1961.

2. Henderson, F.M., Open Channel Flow, 1967.

3. Elevatorski, E.A., Trajectory Bucket Type Energy Dissipators, American Society of Civil Engineers, Irrigation, Pipe Line and Power Division, Vol 84, 1958.

4. Chee, S.P., Padiyar, P.V., Erosion at the Base of Flip Buckets, The Engineering Journal, Volume 52/11, November, 1969.

5. Padiyar, P.V., Erosion Below Flip Buckets, Masters Thesis, University of Windsor, Windsor, 1969.

6. Khosla, A.N., Bose, N.K., McKenzie, Taylor, E., Design of Weirs on Permeable Foundations, Publication No. 12, Central Board of Irrigation, India, June 1954.

7. Schoklitsch, A., Prevention of Scour and Energy Dissipation, Translated at the Bureau of Reclamation, Denver, 1935.

8. Laursseen, E.M., and Toch, A., A Generalized Model Study of Scour Around Bridge Piers and Abutments, Proceedings, Minnesota International Hydraulics Convention, September 1953.

9. Ahmad, N., Mechanism of Erosion Below Hydraulic Works, Proceedings, Minnesota International Hydraulics Convention, September 1953.

10. Gunko, F., Burkov, A.F., Isachenko, N.B., Rubenstein, G.L., Solovyova, A.G., Yuditsky, G.A., Hydraulic Regime and Local Scour of Rock Pad below Spillways of High Head Hydroelectric Stations, XI Congress, International Association for Hydraulic Research, Volume 1, 1965.

11. International Association for Hydraulic Research, Volume No. 3, Erosion and Scour Downstream of Hydraulic Structures, 12th Congress, Colorado, U.S.A.

12. Doddiah, D., Albertson, M.L., Thomas, R.A., Scour From Jets, Proceedings, Minnesota International Hydraulics Convention, September 1953.

13. Kennedy, J.B., Neville, A.M., Basic Statistical Methods for Engineers and Scientists, 1966.

14. Langhaar, H.L., Dimensional Analysis and Theory of Models, 1967.

15. Charles, A.D., Straight Drop Spillway Stilling Basin, Proceedings of American Society of Civil Engineers, Journal of Hydraulics Division, Vol 91, 1965.

16. Rhone, T.J., Peterka, A.J., Improved Tunnel-Spillway Flip Buckets, Transactions American Society of Civil Engineers, Volume 126, 1961.

VITA AUCTORIS

1943 Born on September 22, 1943, in Windsor Ontario, Canada.

1962 High School matriculation from Kennedy Collegiate Institute, Windsor, Ontario.

1967 Graduated from the University of Windsor with a Bachelor of Applied Science(Civil Engineering) and accepted as a candidate for Master of Applied Science at the University of Windsor.